SARTORIUS

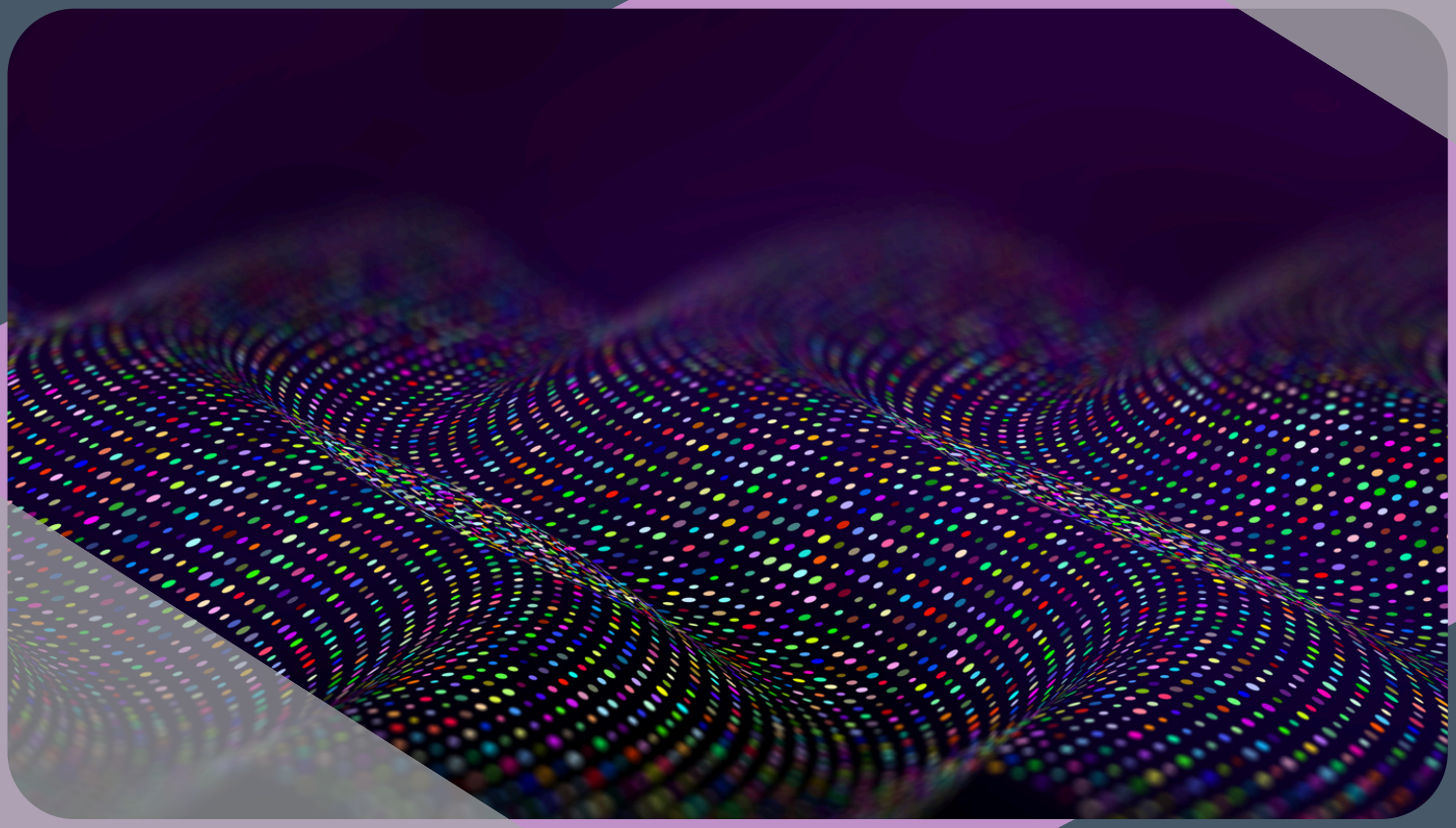

Lab essentials:
Spatial biology

BioTechniques
The International Journal of Life Science Methods

Taylor & Francis

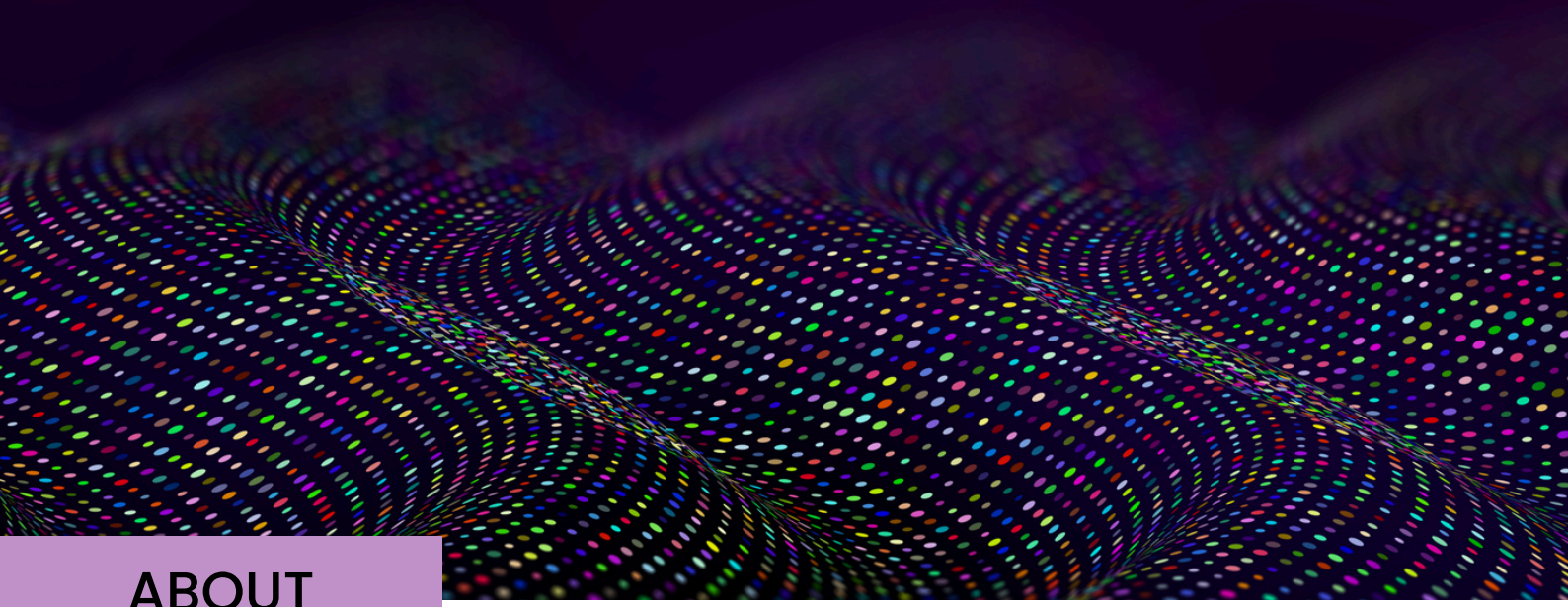

ABOUT

Spatial biology offers unprecedented insights into the complex organization of cells and tissues within their native environments. By preserving and analyzing the spatial context of biological molecules, this field illuminates how cellular location and interactions influence function, development and disease progression. This eBook explores spatial biology techniques, from spatial transcriptomics to proteomics, with key content from *BioTechniques*' digital hub and Taylor & Francis journals.

CONTENTS

Simplifying Progress

Achieve Precision Excellence in Lab Weighing

Discover the Cubis® II Ultra High-Resolution High-Capacity and Semi-Micro balances, designed to deliver unparalleled precision in everyday conditions. Engineered to eliminate performance errors from draft and vibration, these balances ensure accurate measurements every time. With the innovative Cleaning QApp, routine cleanings become effortless, offering step-by-step guidance and an audit trail for compliance.

Request a Demo

SARTORIUS

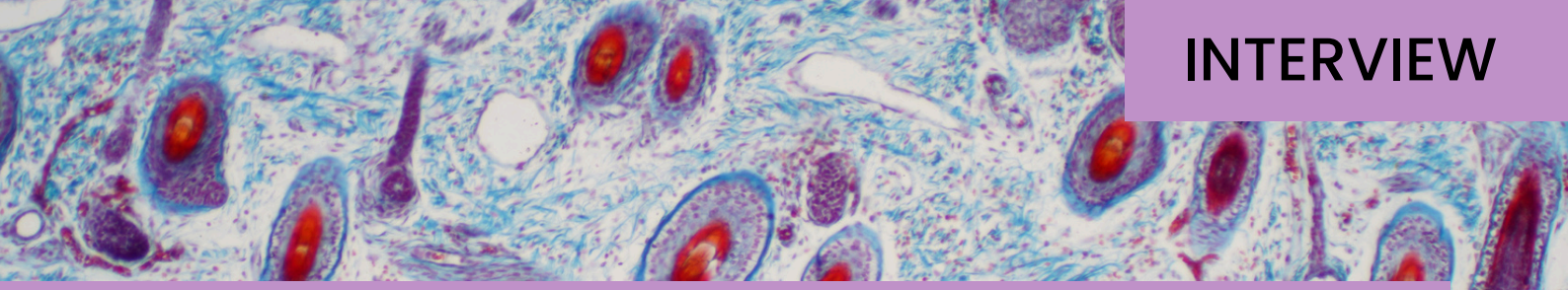

Spatial biology: a collaboration between the biological sciences and information technologies

The first patent for spatial biology was filed in 2000 for a technique called Spatial Analysis of Genomic Activity (SAGA), which received a US patent in 2009. This technique dates back to the 1990s and the launch of the Visible Embryo Project (VEP) [1], which Mike Doyle (now the Vice President of Research at the New Mexico Institute of Mining and Technology, NM, USA) created and led for over 15 years. Here, Mike shares how the VEP led to the advent of spatial genomics and considers the computational advancements that were needed to manage the large datasets required for spatial biology.

What is spatial biology and spatial genomics?

Spatial biology and spatial genomics refer to the study of biological functions and gene expression within their multi-dimensional structural context. This allows us to see where exactly within a tissue or organ certain functions or genes are active.

Spatial biology is just one part of a newly emerging field called spatial science, a field that finds its roots in the development of Geographic Information Systems. The use of spatial science in a variety of fields has enabled researchers to better understand the natural world and to develop new technologies and treatments that can benefit society. These datasets are often highly dimensional and complex, making them difficult to analyze and extract useful information from. However, the potential of these datasets for addressing critical scientific questions is enormous, and the need for new tools and resources for their capture, management, exploration and analysis has become increasingly urgent.

Prior to the rise of spatial biology, researchers could either investigate the biological functionality of specimens or examine their detailed morphological structures, but they could not do both simultaneously. It's reminiscent of a biological version of the Heisenberg Uncertainty Principle: observing the functional aspects of a sample compromised the ability to observe its intricate structural details, and studying the structural details would destroy the ability to observe the physiology.

It is only by visualizing the exact spatial distribution of function-correlated signals within the morphological context of the tissue where these functions occur that researchers can start to decode the intricate spatial interrelationships present in both normal and abnormal biological states. Spatial biology has made this possible.

Could you tell me about the VEP?

In the early 1990s, I was appointed to the oversight committee for a novel initiative by

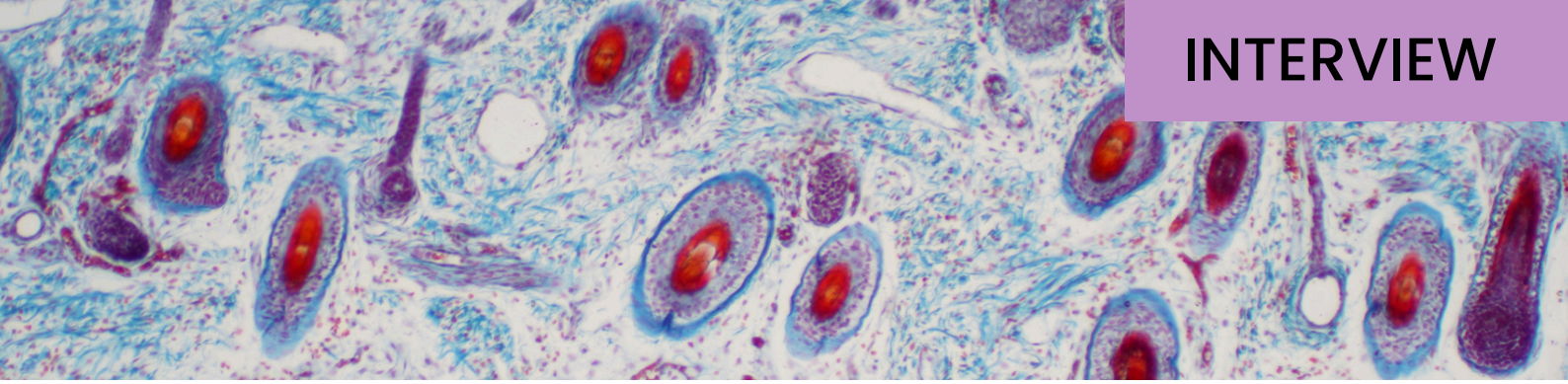

the National Library of Medicine (MD, USA) – the Visible Human Project. This project's objective was to generate an extensive, nationally accessible resource of ultra-high-resolution 3D imaging data on adult human anatomy. I found the prospect of working with such data intriguing. However, it was understood that it would be a few years before any data from the Visible Human Project would be accessible.

Not wanting to wait for the Visible Human Project data, I began seeking other sources of high-resolution 3D images of human anatomy. I came across the Carnegie Collection of Human Embryology at the National Museum of Health and Medicine (Washington DC, USA). The collection consisted of around 650 human embryos, all meticulously sectioned and preserved on slides, which were located at the museum.

This collection bore a striking resemblance to images I had worked with in a project on embryo reconstruction I had initiated during my graduate studies. I realized that if I could devise a way to digitize these sections and reconstruct them in 3D, I would effectively have an image dataset similar to 650 Visible Human Projects. I contacted Adrianne Noe, the Director of the Human Developmental Anatomy Center at the museum, which had recently acquired the collection. She was very excited about the potential of such a venture, prompting me to start creating the necessary tools. Over the following year, Noe and I collaborated on crafting a plan for a large multi-institutional project we called the VEP.

The VEP was initiated with an ambitious aim to deliver real-time 3D visualizations of large high-resolution embryo datasets over the internet, creating a comprehensive online digital archive of multidimensional data on normal and abnormal human development. The motivation was to provide an online interactive environment that would allow researchers from around the world to explore the details and dynamics of embryonic development.

But, through this project, we learned that the scope of biological research can be expanded exponentially by creating and incorporating new technological advances. These advances enabled the integration of both functional and structural information in a way that could provide a comprehensive and interactive new paradigm for exploring biological phenomena.

The biggest lesson? The promise of technology, when wielded thoughtfully, can reshape our understanding of biology in profound ways.

What techniques did you use in the VEP?

We used the first system for spatial biology, which we named SAGA, for Spatial Analysis of Genomic Activity. This involved the basic steps of generating a 3D morphological rendering of a tissue sample, subsampling the tissue along a regular grid pattern, barcoding each subsection sample, analyzing each sample for gene expression and then mapping the gene expression data back onto the morphological rendering of the tissue.

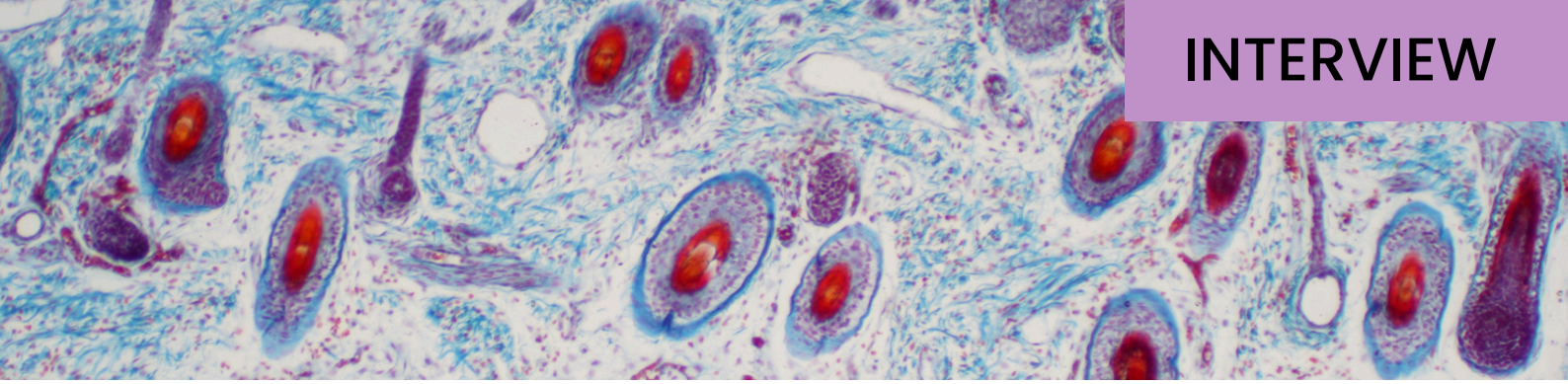

Various methods could be used to accomplish the tissue subsampling. One example we showed involved using sets of alternating serial sections, staining one set for microscopic imaging and using the alternating set for what we called 'tissue rasterization'. This involved incising a regular grid pattern across each tissue section using a laser, and then robotically isolating each square of the grid (each subsample), to a uniquely coded isolation tube for lysis and further processing. Each tube would be barcoded to indicate the x,y,z tissue space coordinate of the original morphological matrix location of the sample.

Each subsample would then go through RNA amplification using reverse transcription, PCR and cDNA microarray analysis. Computer-based image acquisition, processing and analysis would then be used to quantify the strength of fluorescent signals from the microarrays and the resultant gene expression data would be mapped onto the original morphological matrices of image data. The resultant expression-annotated spatial reconstructions could then be used to elucidate biological function, multiplexing the visualization of the expression activity of an enormous number of genes within individual morphological reconstructions.

Together with my three SAGA co-inventors, Maury Pescitelli (University of Illinois Chicago, IL, USA), Betsey Williams (Harvard University, MA, USA) and George Michaels (George Mason University, VA, USA), we filed the first provisional US Patent application for this system on July 28, 2000. The related patent was eventually granted on November 3, 2009 (7,613,571). [2] The patent described the first system for multidimensional mapping of gene expression within tissue morphological context – a concept we dubbed 'Spatial Genomics'. The SAGA patent specification described the foundation for what later became known as spatial transcriptomics and laid out a roadmap for others to follow in the future.

Were there any technological challenges in collecting and storing such large quantities of data in the 90s?

During the project, we had to innovate and develop entirely new technologies to overcome limitations, creating tools where none existed before. For instance, we created a unique web browser that allowed for interactive applications to be embedded directly into web pages. This enabled users to easily access and interact with our complex datasets, even from extremely low-powered personal computers over dial-up connections. We also created the first web cloud architecture, a concept that was over 15 years ahead of its time, to manage and process the large and complex datasets of the project.

This was driven by the challenge of the vast size of the VEP datasets, and the computational complexity required for users to interactively explore the data. The PCs of the early '90s, significantly less powerful than today's machines, stood no chance of managing the colossal embryo datasets that our site aimed to deliver. Back in the

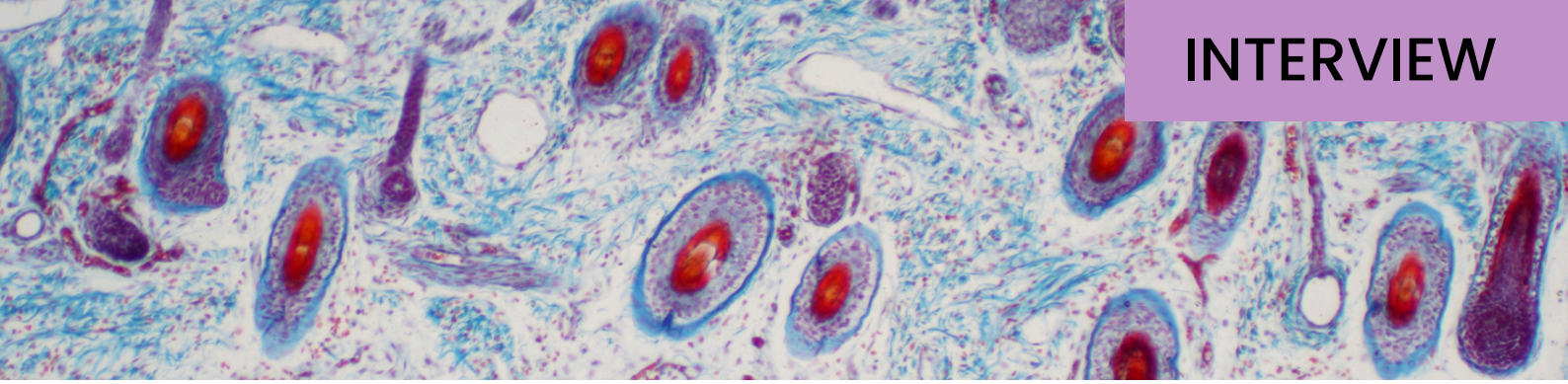

early 90s, the challenges of handling such large datasets were immense. Personal computers were not powerful enough, and internet speeds were extremely slow. To overcome this, we developed a distributed architecture system – today known as 'the cloud' – where a part of a large distributed application would run within the web page and tap into vast computational server capabilities located remotely across the web. This strategy allowed us to bypass the limitations of the local hardware and handle our enormous embryo datasets effectively.

The cloud proved to be a crucial resource for the emergence of spatial biology in the '90s, and it remains so today. Regardless of the computing power one can have on a desk, the ability to tap into the enormous computational and knowledge resources of the cloud allows for greater accomplishments, higher-resolution reconstructions, more complex analyses and the ability to address larger research questions.

How did the VEP lead you to spatial genomics?

The VEP was the first step towards the concept of spatial biology as we know it today. As we started mapping functional data onto 3D images of embryo specimens, we realized that we could extend this idea to a larger scale – to map genomic activity within a tissue or an organism. This led us to the concept of spatial genomics where we combined genomics data with spatial information, creating a holistic view of gene expression within the structural context of tissues.

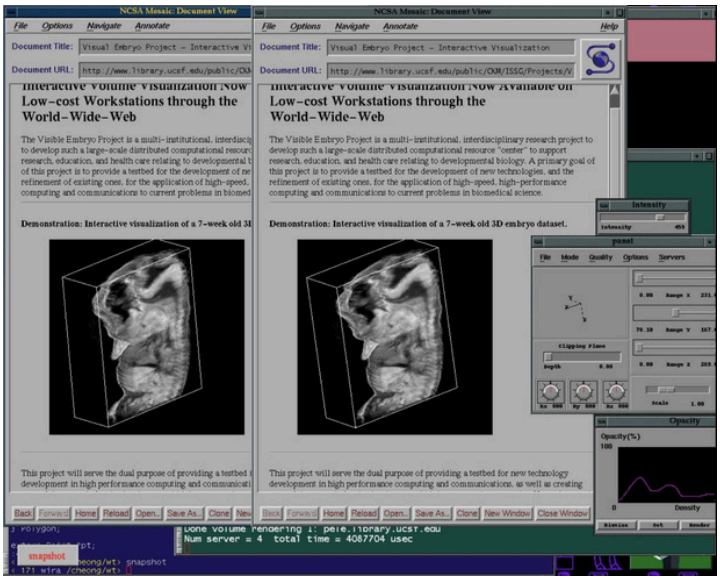

Screen capture of the VEP cloud system from 1994, courtesy of Mike Doyle.

The primary goal of the project, as outlined in the initial plan, was to develop software strategies for creating distributed biostructural databases using state-of-the-art high-performance computing and communications (HPCC) technologies and to apply these tools to construct a comprehensive digital archive of multidimensional data on normal and abnormal human development.

In my lab, one recurring theme was the construction of biostructural knowledge bases that could consolidate functional and structural information about various organisms. So, from the outset, one of the primary objectives of the VEP was to find methods to map biological function data onto multidimensional images of embryo specimens, effectively creating a spatial representation of genomic activity within a tissue morphological framework.

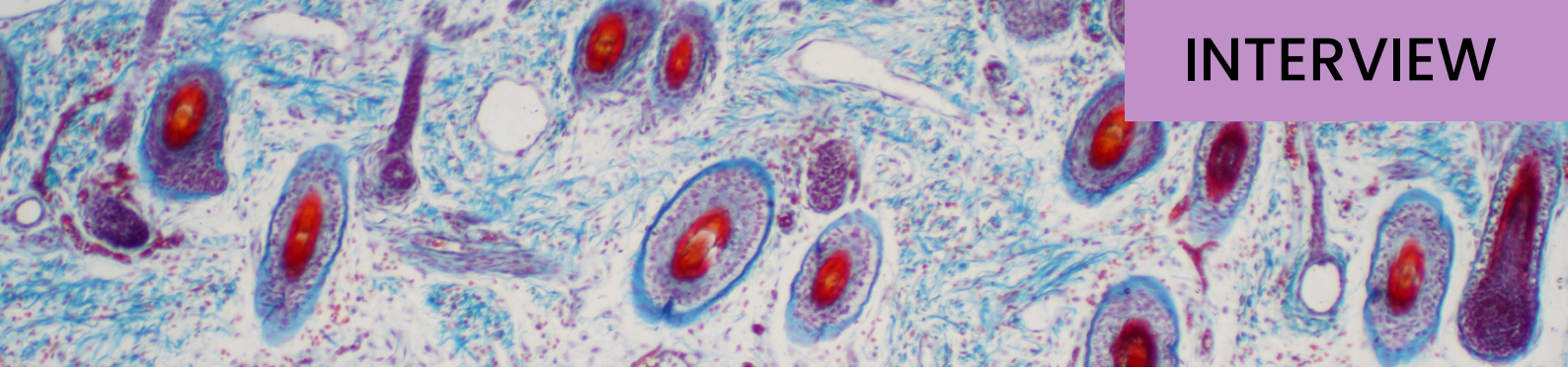

The SAGA system was our "Eureka!" moment for spatial biology. As we mapped functions onto 3D embryo structures, it was as if a light bulb went off. Why not expand this? Why not map gene activity within an entire organism or tissue? This gave birth to spatial genomics – a panoramic view of the expression of tens of thousands of genes, nestled within their structural homes, opening the door to a richer understanding of life's complex interplay.

What are some exciting advancements in spatial genomics in the 23 years since you filed for the patent?

Over the past two decades, the field of spatial biology has seen tremendous growth and innovation, like a flower blooming, each petal revealing another beautiful layer of complexity. The emergence of technologies like single-cell transcriptomics, which break through the cell-resolution barrier enabling imaging of subcellular phenomena, are amazing examples. They will certainly stimulate new waves of research aimed at understanding biological function at unprecedented levels of detail. I can't wait to see what fascinating questions this new lens will help us explore.

Spatial biology's journey from its origins in the VEP to the latest advancements has been a testament to the power of interdisciplinary collaboration between the biological sciences and information technologies.

To move the field forward, at New Mexico Tech we are leading an effort to establish a National Center for Spatial Science (NCSS), which will be a state-of-the-art research center for the development of high-performance computational and algorithmic tools, resources, applications, knowledge and training focused on the advanced analysis of highly dimensional spatially distributed data across a wide range of disciplines. The NCSS aims to facilitate and advance cutting-edge research that requires analyzing large, complex spatial datasets and develop novel methods and techniques for data acquisition, storage, analysis, access and visualization, creating synergies that will benefit all of these fields.

I find myself reflecting on this extraordinary dance between biology and information technology that has spanned over two decades. From its birth in the VEP to the breathtaking advancements of today, spatial biology has led to a riveting symphony of discovery. The upcoming crescendo, I believe, will unveil even more remarkable insights about life's intricate tapestry. Let's keep the music playing.

Sources

1. Doyle MD, Ang C, Raju R et al. Processing of cross-sectional image data for reconstruction of human developmental anatomy from museum specimens. ACM SIGBIO Newsletter 13(1) 9–15 (1993).
2. Doyle MD, Pescitelli MJ, Williams BS and Michaels GS. Method and system for the multidimensional morphological reconstruction of genome expression activity, U.S. Patent 7,613,571, application filed 7/28/2000 (2009).

Machine learning approaches for spatial omic data analysis

Jeremy Goecks is the Assistant Center Director for Research Informatics at the Moffitt Cancer Center (FL, USA), where he is also an Associate Faculty Member in the Department of Machine Learning. Jeremy's computational research lab leads the development of machine learning-based models for the analysis of spatial omic data.

We caught up with Jeremy at AACR 2024 to discuss his lab's work, get best practice tips for collecting and analyzing spatial omic data and discuss how the field can progress in the future.

What did you present at AACR?

I had two stories that I shared with the audience. The first covered our publication detailing the use of spatial omics and machine learning to understand how a novel immunotherapy, agonistic CD40, impacted the tumor microenvironment in pancreatic cancer. We also used these approaches to explore how well we could predict which individuals would respond to that immunotherapy and have long disease-free survival and vice versa. The second story is about how we can develop software to make it easier to run these types of complex analyses, whether you're an experimental or computational investigator.

What were three key takeaways from your presentation?

Number one is that team science is really important. The publication that I shared with the audience was a fantastic collaboration between myself and several immunologists at Oregon Health & Science University including Katelyn Byrne and Lisa Coussens. The combination of my data science expertise and their expertise in immunology was really important in making the project a success.

Takeaway number two is that there are so many different things that you can measure from a single-cell perspective and from a spatial perspective in these tumors that it's hard sometimes to know which features are important. Machine learning is one way that you can get that information and identify which features are helping us understand what's happening with a tumor's biology.

My lab has demonstrated that machine learning can be used to identify which features of the many thousands that you can measure are important, both for understanding how the therapy is modifying the tumor microenvironment and what features are important for predicting response.

The third is that these data science experiments are hard to run and take a long time. We need to build better software to accelerate that process, reduce the amount of time it takes to run these analyses while

ensuring that they're robust, reproducible and useful to the scientific community.

What are your best practice tips for getting the most out of spatial omics data?
One of the first things you need to do is harmonize all the data and metadata available. You want to create a dataset where all the data has been processed in the same way and has the necessary associated metadata, so you know if you're missing anything and exactly where each data point comes from, including which patients and at which time points.

From a data science perspective, best practices focus on reproducible approaches; whether that's GitHub to store your code or using automated pipelines to run your analyses and produce figures. This means when the time comes to reproduce that analysis or apply it to a new data set, you're able to do so, confident that you are repeating the analysis exactly.

What exciting contributions has your lab made to spatial omic data analysis?
We are trying to use machine learning to improve both our ability to predict a therapeutic response and our understanding of the underlying biology that leads to said response. We can interrogate our models to find out why they made a specific prediction and identify which biological features they are using. This avoids the typical 'black box' issue of a lot of AI models, where they answer a question but can't explain how they arrived at the answer.

The other major contribution is trying to keep the models as simple as possible. We use relatively simple machine learning models but are still able to demonstrate good performance on our data sets. You don't always need the most complex algorithms in order to get the signal out of the data if the data set is strong.

What can researchers do at the data generation stage to help improve their downstream analysis?
I always encourage my experimental colleagues to make sure that they record all the elements of their experiment. Everything from the antibodies and sample IDs to the particular microscopy focal levels used. All the metadata that they have available should, to the best of their ability, be recorded in a systematic way.

The second thing I think is relatively straightforward, but it's to try to process all your samples in the same way. If you process your samples in the same way, it's much easier to computationally analyze them and not worry that there are technical differences that are coming out in the analysis rather than the biological differences that you really want.

If there was one thing you could ask for to maximize the impact of spatial omics data in cancer, what would it be?
I would say sharing more of these datasets widely, from the raw images to the downstream single-cell omics tables, would be at the top of my list. Making this data open would allow other analysts to come and put their hands on it, to connect it with other data sets, and these larger data sets ultimately, I think, is how we will accelerate cancer research and improve patient care as a community.

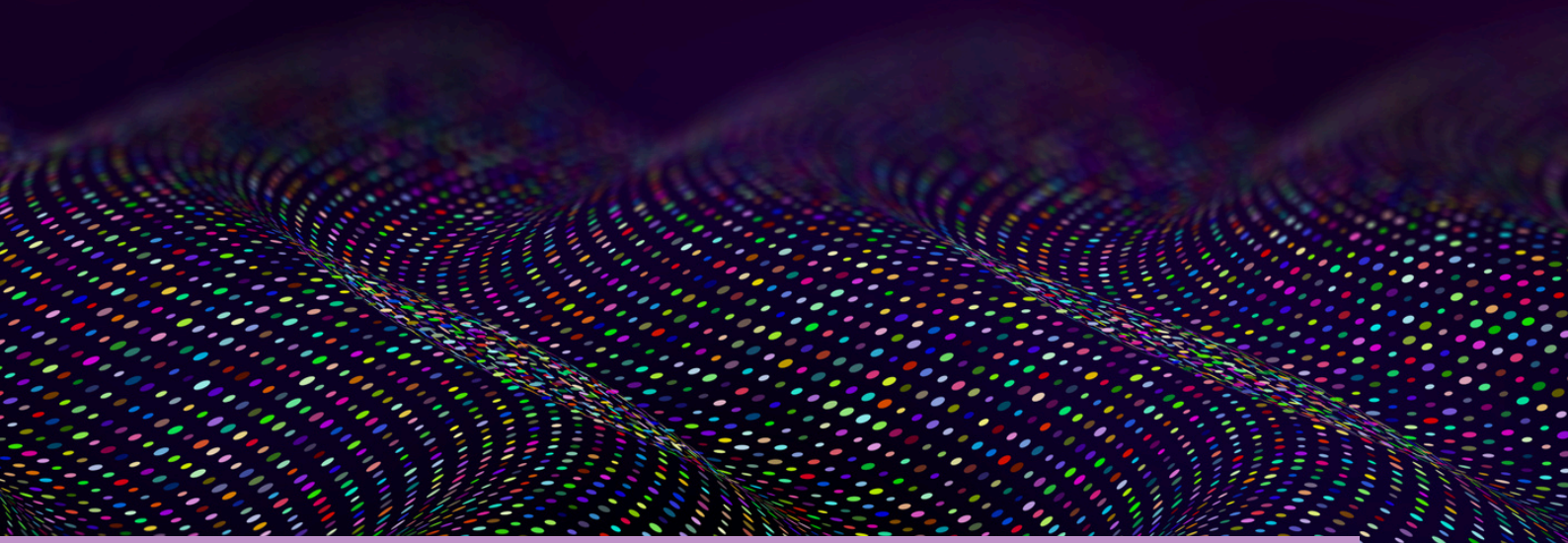

The link between spatial biology and lab weighing

Lab balances are essential for spatial biology research. Precise weighing is crucial for preparing samples, reagents and conducting experiments that require accurate quantification of biological materials. Lab balances ensure that these measurements are reliable, which is vital for the integrity of spatial biology experiments and analyses. Accurate weighing supports the experimental processes that enable spatial biology research, contributing to the validity and reproducibility of the findings.

Environmental factors such as static electricity and magnetism can significantly impact the accuracy of lab balances, leading to potential errors in measurement. Static electricity can cause fluctuations in weight readings, while magnetism can influence the balance's sensitivity and stability. These factors are critical in spatial biology, where precise quantification of biological materials is essential for reliable data collection and analysis. Understanding and mitigating these environmental influences ensures the integrity of spatial biology experiments, thereby supporting the accurate study of cellular organization and interactions within their native environments.

Read more about the effects of static electricity and magnetism on analytical weighing in the following resources from Sartorius.

SARTORIUS

Application Article

March 30, 2020

Keywords or phrases:
Electrostatic Influences, Analytical Balances, Lab Weighing

Effects of Static Electricity on Analytical Weighing

Introduction

Among the various options for eliminating static electricity during analytical weighing, there are simple, low-cost measures available. However, due to the current metrological and practical limitations, many of these measures are difficult and time-consuming to use and are not universally applicable. On the other hand, there are methods that are both powerful and space-saving, particularly when they are integrated directly into the balance.

Static electricity is a physical phenomenon that is a common occurrence in many areas of our daily lives, and it can have tremendous significance in industry and all kinds of research and development laboratories. Electrostatic charging of materials, for instance, in industrial processes and during production sequences or materials analysis can have negative effects. For example, dosing powders with a spatula or dosing heads risks spreading the substance so it cannot be brought into the vessel without spilling. Electrostatic discharges can damage electronic equipment and components. Spark discharges can easily ignite flammable substances in the immediate vicinity, which, for example, can lead to serious accidents. Thus, millions of dollars are spent around the world on efforts to eliminate electrostatic charges and their associated negative effects.

Basics of Static Electricity

Static electricity results from friction between two objects (bodies). This friction process transfers electrons from objects with a lower work function (donator) to objects with a higher work function (acceptor), which results in the production of ions (see Fig.1). A body with excess electrons takes on a negative charge, while a body lacking electrons takes on a positive charge. However, this is only a temporary change in the charge because any excess electrons flow off of the body once it has a certain conductivity or is grounded.

Friction can occur within the sample itself or between the sample and container or tare vessel. For example, during convection in a drying oven, air friction creates a charge on glass containers, and internal friction of powders and liquids when they are transferred between containers creates a charge on particles within that sample. In practice, it is impossible to avoid friction during the processing or transport of substances. Thus, electrostatic charging occurs nearly 100% of the time. Disruptive electrostatic forces can also occur in the area around the balance, due to the direct transfer of charge carriers by people moving around the balance.

Direct Impact on Weighing

All balance manufacturers are called upon to respond to the problems of weighing substances with electrostatic charges with appropriate technological solutions. Static electricity can have a negative effect on either the weighing process itself or on the results, thus requiring time-consuming material selection or material handling procedures to address these effects. In some cases, weighing a material may be close to impossible due to the build-up of electrostatic charges during handling. In addition, the electrostatic properties of some materials may vary as ambient humidity rises and falls, making the attempt to weigh it even more difficult. Often, electrostatic phenomena are worse when the relative humidity falls below 45%–which is often the case in winter in European latitudes or in air-conditioned rooms. Therefore, balance users will experience different conditions from one season to the next or from one day to the next, making it difficult to reproduce their results.

Electrostatic charging of materials can occur in the following conditions:

- in solids, when the surface resistance of the material Rs > 10 GΩ (according to IEC93)
- in liquids, with a conductivity of < 10 nS/m
- in conductive materials that are not grounded

During a weighing operation, the interaction of electrical charges that have built up on the material being weighed and the fixed parts of the balance, which are not conductively connected to the weighing pan, cause this electrostatic force.

An electric field, thus, builds between the material being weighed and the fixed parts of the balance. Some examples of fixed balance parts include the draft shield or housing parts, such as the balance base plate.

The resulting electrostatic forces can cause load changes (displayed values) up to the order of a gram. In practice, a false absolute weight is not the only negative effect associated with static electricity. Severe drift of weight readouts and poor repeatability of results are also serious problems.

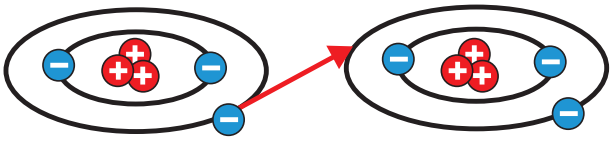

Figure 1a:
Schematic illustration of ion creation: When two neutral atoms collide or experience friction, the body with the lower work function loses an electron.

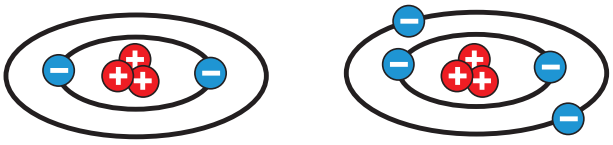

Figure 1b:
The lost electron moves to the body with the higher work function, and an ion is created.The total charge of the atom on the left is positive (positive ion); the total charge of the atom on the right is negative (negative ion).

Built up charges flow off slowly via the weighing pan, so that the resulting forces are not constant over time, causing drift and poor repeatability. Depending on the polarity the charge carries, the interaction can be either repulsive or attractive, meaning the weight results can deviate both positively and negatively.
A repulsive interaction occurs when both the charge on the sample and the ambient charge have the same polarity (both + or both –) (see Fig. 2). The material being weighed seems heavier than it actually is.

An attractive interaction, on the other hand, occurs when the charge on the sample and the ambient charge have different polarities (one + and one –). An attractive interaction will, thus, make the material being weighed seem lighter than it actually is (see Fig. 3).

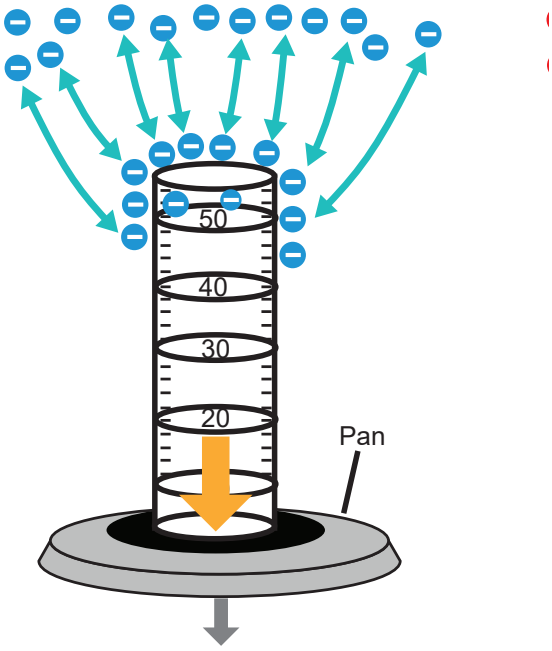

Figure 2: Repulsive interaction during weighing. When both the weighing container and the environment are negatively charged, the resulting force is directed downward (yellow arrow). This makes the sample appear heavier.

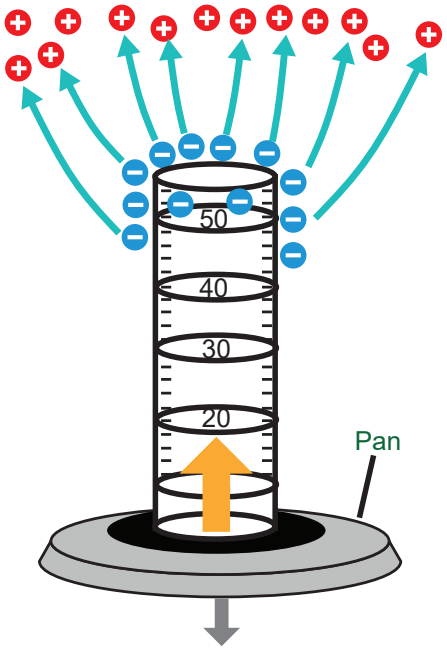

Figure 3: Attractive interaction. When the weighing container and the environment have opposite charges, the resulting force is directed upward (yellow arrow).This makes the sample appear lighter.

Neutralizing Electrostatic Charges

To eliminate the effects of static electricity on weighing, keep both the sample and the area around it free of any charges. One method that has yielded excellent results to shield the weighing chamber and the weighing pan from electrostatic fields is to use a fully transparent conductive coating on all glass elements of the balance draft shield. All glass draft shields of the Cubis® II series include this important feature.

Another solution includes using ionizers and anti-static pens near the balance (see Fig. 4). This solution works on the principle of surface neutralization via ion bombardment. In most situations, surface neutralization is very effective at reducing charge buildup when it is helpful to eliminate electrostatic charges on vessels and samples in the external environment of the balance.

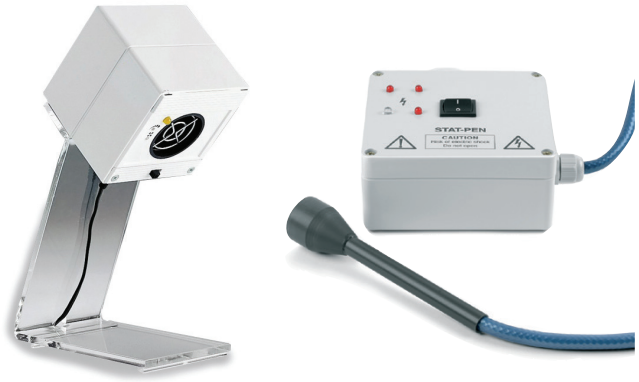

Figure 4: Ionizer and anti-static pen

Below-balance weighing can be used for weighing bulky materials, such as plastic blocks. The sample is secured using a hanger beneath the weighing pan to take advantage of the proportional reduction in electrostatic force that occurs with the square of the distance between the charge carriers. Of course, this method of reduction of the influence of electrostatic charges can also be used while weighing on the weighing pan; any influence of electrostatic forces on weighing results can be reduced if the distance between the sample and the weighing pan is significantly smaller than the distance between the sample and the fixed parts of the balance because the weighing pan provides an effective shield. However, if the opposite is true, electrostatic charges will still affect the weighing process. Sometimes it is sufficient to place an object between the sample and the weighing pan, reducing the forces to the point that they have no noticeable effect on the weighing result. For some applications, it is also enough to increase the shielding effect of the weighing pan. For this purpose, special pans (Figure 5) with a greater diameter than standard pans are offered.

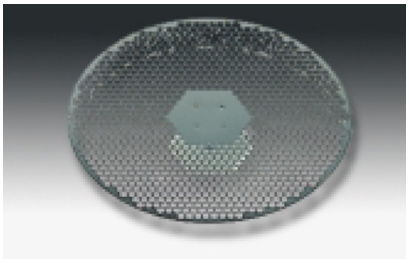

Figure 5: Anti-static weighing pan for improved shielding of electrostatic charges from samples. Designed as a perforated disk to reduce its weight, this pan style is used primarily for weighing filter materials.

Figure 6 shows an example of a specific balance for weighing filters which uses a Faraday cage (a grounded metal shield) to solve the problem of electrostatic charges. While weighing, the weighing pan and an electrically conductive cover attached to the pan shield the filters completely. This filter weighing balance is often used to determine particulate matter in emission measurements in the automotive industry or environmental institutes.

Figure 6 : Cubis® II Micro balance with special draft shield M for weighing filters of sizes up to 90mm.

Useful Equipment to Avoid Influences of Electrostatic Charges

Generally, the time needed to neutralize electrostatic charges depends on the material, surface, and shape of the sample, as well as the relative humidity in the vicinity of the balance.

The new Cubis® II balance offers the Q-Stat ionizer, which is integrated in the draft shield I of the modular balance series and eliminates electrostatic charges within a few seconds.

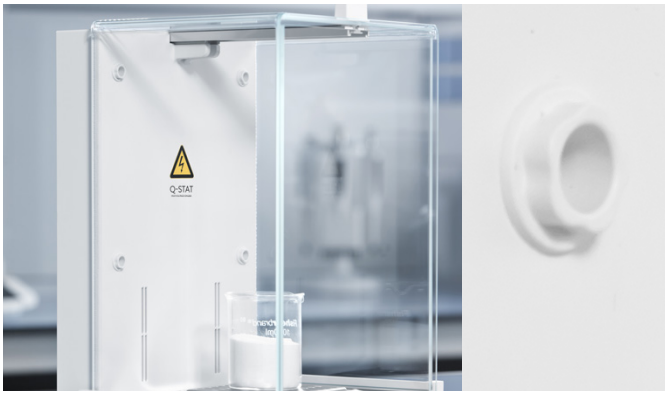

Figure 7: The Cubis® II motorized automatic draft shield I includes an ionizer with four jet nozzles for effective elimination of electrostatic charges.

In the draft shield I of the Cubis® II, four nozzles jets are positioned in the rear wall (see Fig. 4). The physical functional principle of these nozzles is Corona Discharge, a process by which a current flows from an electrode with a high voltage into the air. Around the very thin needle, the electric field strength is so high, that the air molecules are ionized and create a region of plasma around the electrode. The generated ions pass the charge to areas of lower potential. After recombination with free charges they form neutral gas molecules again.

The use of four nozzles in the Cubis® II balance makes charge elimination very effective. By using opposite polarity of the nozzles, a kind of focusing effect in the area of the weighing pan occurs. This makes the neutralization of electrostatic charges from sample containers and substances, for instance, powders, very effective without disturbing airflows. This prevents errors from electrostatic forces in the weight measurements.

Moreover, the fully transparent conductive layer on the draft shield glass panels of this models provide additional protection from electrostatic fields in the immediate proximity of the balance. This too ensures stable and correct weighing results independently of electrostatic charges.

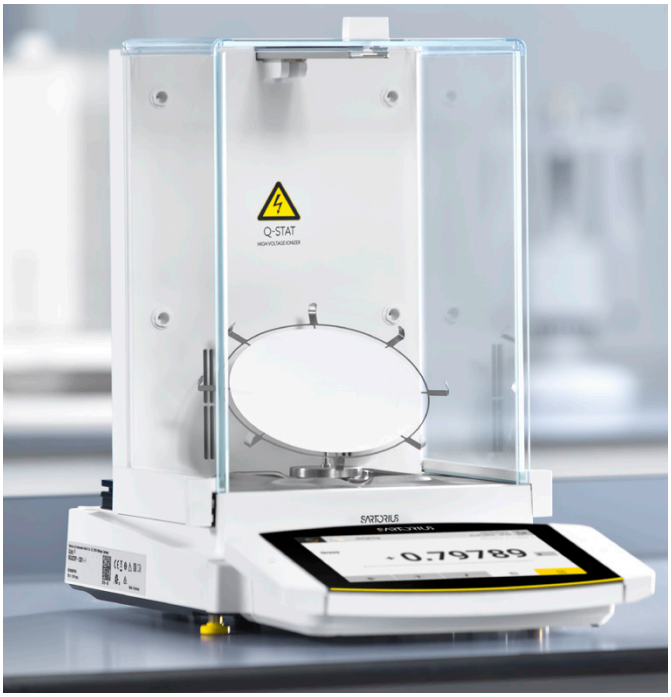

Figure 8

Cubis® II supports different applications in which an elimination of electrostatic charges is essential to measure very small amount of particles on filters (here with special holder YSH30 for filter diameters up to 150mm).

SARTORIUS

White Paper

May 13, 2020

Keywords or phrases:
Magnetism, High-resolution Weighing, Environmental Influences, Titanium Weighing Pan, Cubis® II Micro Balance

Magnetism—an Influencing Factor on Weighing

Dr. Thomas Pertsch
Sartorius Lab Instruments GmbH & Co. KG, Otto-Brenner-Straße 20, 37079 Goettingen

* Correspondence
E-Mail: lab-requests@sartorius.com

Abstract

Magnetism and electricity are natural phenomena, which have been known since ancient times. In 1820, Danish physicist Hans Christian Oersted noticed that a compass needle was deflected when held near a wire through which an electric current flowed. He concluded that a current-carrying conductor is surrounded by a magnetic field that affects the compass needle. Today, the interaction of electricity and magnetism is explained using an elegant physical theory summed up in the Maxwell equations.

In the industrial age, the importance and use of magnetism and magnetic materials grew, most notably through the development of electric motors. Nowadays, it would be hard to imagine life without the benefits of magnetic effects and the use of magnetic materials; for example, digital data are saved onto magnetic media like the computer hard disk, and electric motors are beginning to compete with gasoline engines. However, magnetism is an unwelcome phenomenon during weighing.

How Does Magnetism Influence Weighing?

Despite the positive benefits of magnetism, it is a rather unwelcome phenomenon during weighing. Weighing magnetic materials or magnetizable tare vessels or samples may destabilize the weight result or compromise repeatability. For example, when weighing a sample or vessel containing iron, steel, cobalt, or nickel, users may see the following effects:

- Weight values are stable, but non-repeatable
- Different values are displayed, depending on the position of the sample on the weighing pan

These effects may be from one of two causes:

1. If the material to be weighed is magnetized, such as a stirring rod of a magnetic stirrer, the weight force of the sample is superseded by the attractive force its magnetic field exerts on the magnetizable parts of the weighing chamber or weighing cell.
2. If the weighing cell is designed on the electromagnetic force compensation principle, a strong magnet is used in this system. Despite careful shielding measures of the magnet, the balance is surrounded by a low residual magnetic field, and this residual field can influence the weighing result if interaction occurs with the sample or vessel.

Figure 1 illustrates the field pattern of magnetic or magnetizable samples. Here, these magnetic forces, and their influence on the weight result, are strongly dependent on the orientation of the sample in the field of disruption. The influence of magnetic forces is stable over time and is often only detected on the basis of repeated weighing, because different weight results are generally obtained as a result of varying the position and orientation of the sample on the weighing pan. Thus, this factor poses a latent negative influence on the accuracy of the weighing result.

One simple and effective solution to address the magnetic influence on weight results is to increase the space between the material being weighed and the weighing cell. This works because the magnetic interaction has a quadratic dependence on the distance from the material being weighed. The distance can often be increased by simply placing a piece of glass, wood, non-magnetic metal, or plastic between the weigh cell and the sample.

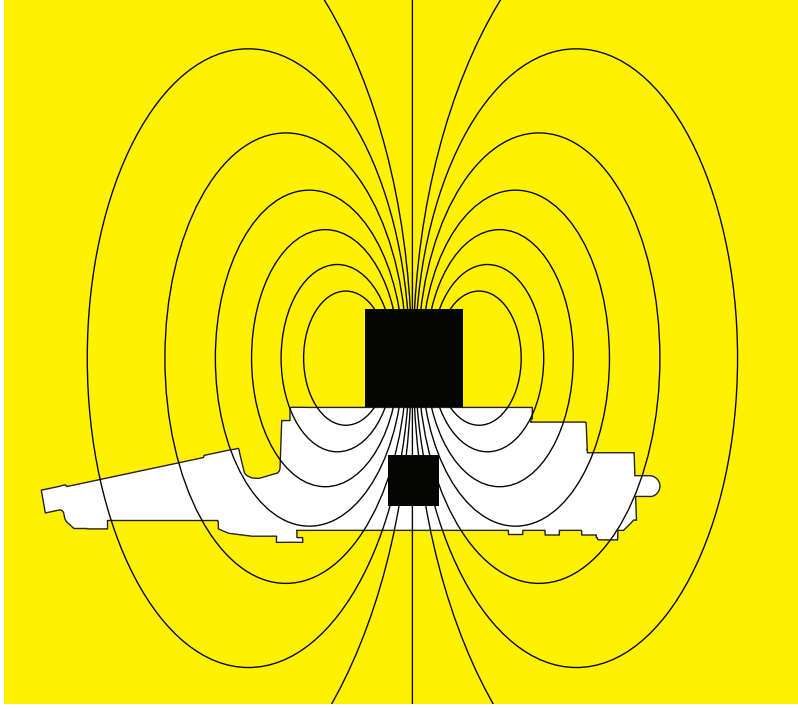

Figure 1: Field pattern of magnetic or magnetizable samples

Figure 2: Below-balance weighing for magnetic samples with an Entris II precision balance

Figure 3: Cubis® II micro balance with titanium pan and inner draft shield parts

Figure 4: Titanium vial holder for a Cubis® II semi-micro balance reduces magnetic influences

If this cannot be done because a bulky material is to be weighed, the principle of below-balance weighing is another option (Figure 2). In this case, to increase the distance between the material and the weighing pan, the material being weighed is secured underneath the weighing pan using a hanger designed for below-balance weighing.

Likewise, if the distance cannot be increased due to space constraints, shields of soft magnetic materials can be used to rectify this problem. These shields are created from highly permeable nickel iron alloys (known as Mu-metal) and are available in different shapes, such as foils, plates, or tubes.

If there are problems with weighing of magnetic samples or vessels, the above options can help, but the best solution is to use a balance specially designed to address problems with magnetism. For instance, the modular Cubis® II premium laboratory balance series has weighing pans made of non-magnetic titanium for all higher-resolution models, starting with analytical balances.

Moreover, Cubis® II ultra-micro and micro balances have both a weighing pan and a draft shield base plate (Figure 3) of titanium, to reduce the destabilizing magnetic influence when weighing samples or tare vessels containing iron, cobalt, or nickel.

An additional problem may occur with the orientation of a stainless steel sample holder, in the case that a special sample holder (see Figure 4 and Figure 5) is used for specific customer applications, for example weighing reaction vials, reaction tubes, or filters. If the sample holder is rotated, for example, to achieve a better positioning for dosing of small powder amounts, the orientation of the magnetic fields changes and thus the weight value could be influenced. The same effect could also occur if the round stainless steel pan of an ultra-micro or micro balance is slightly rotated.

Figure 5: Titanium sample holder for Cubis® II reaction tubes or flasks of different sizes

However, with parts made of titanium this cannot happen. As mentioned previously, all sample holders for Cubis® II are made from the highest quality titanium and thus deliver the highest reliability of weighing performance and results, and a high grade of corrosion resistance.

Conclusion

This white paper describes the influences of the physical effect of magnetism on high-resolution weighing. The type of influences are described and the possibilities mentioned to recognize them in daily use of the balance. In particular, practical instructions are given on how the influence of magnetism can be avoided or reduced.

In addition, the measures provided by the manufacturer in high-resolution balances are described. The use of weighing pans, sample holders, and parts inside the draft shield, made from the non-magnetic and non-corrosive titanium, offers an innovative and effective solution.

Sales and Service Contacts

For further contacts, visit www.sartorius.com

Germany
Sartorius Stedim Biotech GmbH
August-Spindler-Strasse 11
37079 Goettingen
Phone +49 551 308 0

USA
Sartorius Stedim North America Inc.
565 Johnson Avenue
Bohemia, NY 11716
Toll-Free +1 800 368 7178

Taylor & Francis
Taylor & Francis Group

Expert Review of Proteomics

ISSN: 1478-9450 (Print) 1744-8387 (Online) Journal homepage: www.tandfonline.com/journals/ieru20

Spatial Proteomics towards cellular Resolution

Yumi Kwon, James M. Fulcher, Ljiljana Paša-Tolić & Wei-Jun Qian

To cite this article: Yumi Kwon, James M. Fulcher, Ljiljana Paša-Tolić & Wei-Jun Qian (2024) Spatial Proteomics towards cellular Resolution, Expert Review of Proteomics, 21:12, 505-514, DOI: 10.1080/14789450.2024.2445809

To link to this article: https://doi.org/10.1080/14789450.2024.2445809

EXPERT REVIEW OF PROTEOMICS
2024, VOL. 21, NO. 12, 505–514
https://doi.org/10.1080/14789450.2024.2445809

Taylor & Francis
Taylor & Francis Group

SPECIAL REPORT

Spatial Proteomics towards cellular Resolution

Yumi Kwon [a], James M. Fulcher [a], Ljiljana Paša-Tolić [a] and Wei-Jun Qian [b]

[a]Environmental Molecular Sciences Laboratory, Pacific Northwest National Laboratory, Richland, Washington, USA; [b]Biological Sciences Division, Pacific Northwest National Laboratory, Richland, Washington, USA

ABSTRACT

Introduction: Spatial biology is an emerging interdisciplinary field facilitating biological discoveries through the use of spatial omics technologies. Recent advancements in spatial transcriptomics, spatial genomics (e.g. genetic mutations and epigenetic marks), multiplexed immunofluorescence, and spatial metabolomics/lipidomics have enabled high-resolution spatial profiling of gene expression, genetic variation, protein expression, and metabolites/lipids profiles in tissue. These developments contribute to a deeper understanding of the spatial organization within tissue microenvironments at the molecular level.

Areas covered: This report provides an overview of the untargeted, bottom-up mass spectrometry (MS)-based spatial proteomics workflow. It highlights recent progress in tissue dissection, sample processing, bioinformatics, and liquid chromatography (LC)-MS technologies that are advancing spatial proteomics toward cellular resolution.

Expert opinion: The field of untargeted MS-based spatial proteomics is rapidly evolving and holds great promise. To fully realize the potential of spatial proteomics, it is critical to advance data analysis and develop automated and intelligent tissue dissection at the cellular or subcellular level, along with high-throughput LC-MS analyses of thousands of samples. Achieving these goals will necessitate significant advancements in tissue dissection technologies, LC-MS instrumentation, and computational tools.

ARTICLE HISTORY
Received 16 August 2024
Accepted 13 December 2024

KEYWORDS
Laser-capture microdissection; mass spectrometry; nanoPOTS; spatial omics; proteomics; single-cell proteomics; spatial biology

1. Introduction

The behavior of multicellular organisms is governed by the intricate molecular organization across spatial dimensions. By measuring these dimensions, we can gain detailed understanding of fundamental biological processes in both homeostatic and pathological states, as well as understand how diverse cell types interact to collectively determine tissue functional state. Some unique examples highlighting the importance of single-cell resolved spatial organization include the recent discovery of a fourth meningeal layer in mammalian brains [1] and the importance of pancreatic delta cells in paracrine signaling and glucose homeostasis [2]. In the context of human pathologies, the spatial organization of cells in the tissue microenvironment (e.g. tumor) is known to impact therapeutic response [3], while bystander effects (*e.g.*, a cell's response resulting from an event in an adjacent cell) can be observed in the context of radiation exposure or cellular senescence [4,5]. Thus, spatial characterization of biomolecules within tissue microenvironment holds a great potential for accelerating biological discovery.

Spatial biology is an emerging multidisciplinary field integrating imaging and spatial omics technologies with computational tools for gaining an understanding of the *in situ* spatial cellular organization, cell neighborhoods, and interactions within tissue microenvironment with high-dimensional spatially resolved molecular data. Several ongoing large-scale research programs, such as the Human BioMolecular Atlas Program (HuBMAP) [6] and the Human Tumor Atlas Network (HTAN) [7], focus on spatial mapping of biomolecules at cellular resolution in healthy human body and human cancers, respectively, further highlighting the significance of spatial biology.

During the past two decades, global omics approaches for broadly measuring biomolecules have matured considerably, with recent advancements allowing for thousands of measurements from a single-cell [8]. With more recent technological breakthroughs, the spatial dimension has also begun to be captured alongside these omics measurements at or near single-cell resolution [9]. Notably, different modalities with spatial information can be accessed with divergent approaches. For example, spatial transcriptomics (*i.e.*, spatially resolved RNA measurements) can be conducted with fluorescence in situ hybridization (*e.g.*, MERFISH [10]) or barcoding of sequencing reads (e.g. Slide-seq [11], Visium [12], and more recently Visium HD [13] and Stereo-Seq [14]). Mass spectrometry imaging techniques (such as matrix-assisted laser desorption/ionization [MALDI] [15] and gas cluster ion beam imaging [16]) can be used to spatially profile metabolites, lipids, and glycans with near-single-cell resolution. Realizing global spatial proteomics (*i.e.*, spatial mapping of protein abundances with a broad proteome coverage) has proven to be more challenging. Current spatial proteomics techniques mainly rely on affinity reagents (*e.g.*, immunohistochemistry (IHC) or immunofluorescence) and unique tags or barcodes have been introduced to enhance their multiplexing capacities for imaging a targeted

CONTACT Wei-Jun Qian weijun.qian@pnnl.gov Biological Sciences Division, Pacific Northwest National Laboratory, 902 Battelle Boulevard, Richland, WA 99352, USA

Article highlights

- Mass spectrometry-based spatial proteomics is an emerging field that complements other spatial omics techniques, enabling unbiased molecular mapping of tissues.
- The current spatial proteomics workflow is supported by microscale tissue dissection (such as laser capture microdissection), nanoscale sample processing, and advanced LC-MS instrumentation.
- Recent demonstrations of spatial proteome profiling in tissues with near-single-cell or single-cell resolution illustrate the potential of spatial proteomics.
- Key challenges in the current workflows include improving the precision and throughput of tissue microdissection, enhancing the sensitivity of instrumentation for achieving deep proteome coverage, and optimizing throughput for efficient mapping of target areas.
- Future advancements in dissection technologies, LC-MS instrumentation, and computational tools are anticipated to establish spatial proteomics as a foundational tool for biological discoveries.

panel of proteins, including MALDI-IHC tags (AmberGen [17]), spatial cellular indexing of transcriptomes and epitopes by sequencing (CITE-Seq) [18], imaging mass cytometry [19] and CODEX [20]. The multiplexity of antibodies, however, limits the number of proteins that can be measured to a maximum of a hundred depending on the techniques. Direct imaging of proteoforms [21] using MALDI imaging or nanospray desorption electrospray ionization (nanoDESI) obviates the need for antibodies, but these techniques suffer from limited identification depth (up to several hundreds of proteoforms) and are generally (depending on the mass analyzer employed) restricted to proteins with more easily resolved isotopic distributions and favorable ionization characteristics, such as those below ~ 70 kDa [22,23]. Recent advances in bottom-up nanoscale proteomics (or near single cells) and single-cell proteomics (scProteomics) open a potential path for achieving unbiased spatial proteomics toward cellular resolution. This direction is seen as highly promising due to its relatively high identification depth using bottom-up LC-MS workflow and the ability to capture post-translational modifications (PTMs). In this article, we specifically focus on bottom-up MS-based spatial proteomics by presenting a summary of recent advances in the area, discussing the current state-of-the-art of spatial proteomics and its associated challenges, and projecting the future potential of this technological field for biological discoveries.

2. General challenges of MS-based spatial proteomics

Figure 1 illustrates the typical workflow of current bottom-up MS-based spatial proteomics, which consists of three main components: 1) image-guided *in situ* tissue or cell dissection by targeting specific regions of interest (ROI) based on images of pathologic or phenotypic markers; 2) microscale or nanoscale sample processing to minimize protein/peptide loss prior to LC-MS analyses; 3) high-throughput LC-MS analysis and downstream bioinformatics. Recent advances in all these areas have enabled spatial proteome mapping of tissue sections with relatively deep proteome coverage (e.g. >2000 proteins) and near-single-cell resolution [24,25]. Ideally, spatial proteomics should be able to map tissue regions at cellular resolution or even subcellular resolution in a high-throughput fashion such that hundreds of thousands of cells within a tissue section can be mapped similar to those offered by spatial transcriptomics (e.g. Visium HD [13]). However, challenges in implementing these approaches continue to persist, some specific to spatial mapping and others more generally associated with scProteomics. The first challenge has been the ability to perform targeted dissection and capture of small regions of tissue for downstream analysis in an intelligent and automated fashion. Tissue dissection is typically performed through laser capture microdissection (LCM) techniques, which is rather tedious and low throughput. Secondly, the limited throughput of LC-MS measurements is a significant bottleneck for both scProteomics and spatial proteomics, and consequently only limited number of regions have been mapped within limited number of tissues to date. Finally, bioinformatic reconstruction of the spatial dimension, protein abundances, and integration of proteomic data with other

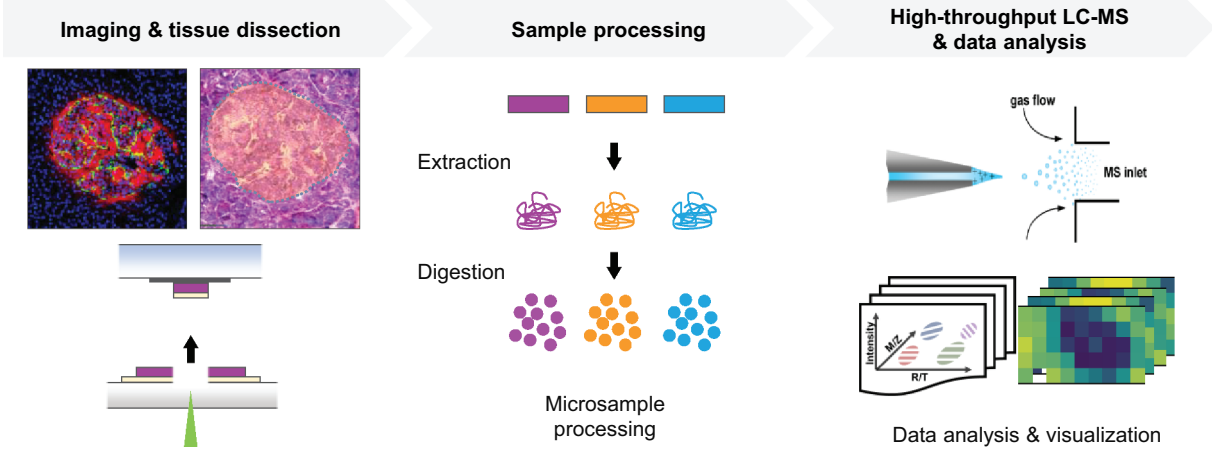

Figure 1. General workflow for LC-MS-based spatial proteomics. The workflow starts with imaging and dissection of specified cell populations from tissue sections, typically using LCM following H&E or immunofluorescence staining. The dissected cells or regions are transferred to a nanoscale sample processing platform such as the nanoPOTS chip for protein extraction, followed by digestion. And nanoLC-MS analysis. The resulting data allow for peptide and protein identification and quantification, enabling the spatial mapping of protein abundances within a sampled ROI and ultimately across the tissue section.

modalities (i.e. through image co-registration) is still an area of active development. Herein, we discuss recent advances in tissue dissection, sample processing, ultrasensitive LC-MS platforms, and bioinformatic developments for spatial proteome mapping in tissues toward cellular resolution. We anticipate that these advances and future developments will pave the way for answering fundamental questions about intercellular spatial organization, communication, and regulation across spatial dimensions.

3. Tissue dissection techniques for spatial proteomics

Since samples cannot be analyzed nondestructively through LC-MS proteomics, precise tissue dissection of specific ROI is essential for facilitating spatial proteomics. Several tissue dissection techniques, including traditional tissue voxelation [26] and LCM, have been developed to facilitate spatial proteomics mapping across a range of spatial resolutions. The ideal tissue dissection technology (Figure 2) should include two key elements: 1) accurate, efficient, and automated tissue microdissection guided by tissue images, potentially in combination with artificial intelligence (AI) algorithms, and 2) streamlined tissue/cell collection without sample loss to facilitate downstream processing.

Conceptually, mechanical methods can be applied to dissect specific regions from solid tissues and subject them to proteome profiling with spatial resolution. The voxelation technique using cutting blades or a 2D array of cutting blades was one of the earliest methods employed for tissue dissection for spatial transcriptomics [27] and spatial proteomics [26]. These techniques involve manually excising specific regions of tissue based on visual cues, allowing for the targeted analysis of distinct anatomical features. While straightforward, these methods can be labor-intensive and offer poor spatial resolution (~1 mm). A micro-scaffold assisted spatial proteomics (MASP) technique that applies 3D-printed micro-scaffolds to tissues, however, represents an improved dissection approach relative to these manual methods [28]. In MASP, preservation of spatial information is achieved by pressurization of a 3D-printed micro-scaffold containing precisely spaced cubicles that are pressed against the tissue for compartmentalization. A related μDicer technique consists of

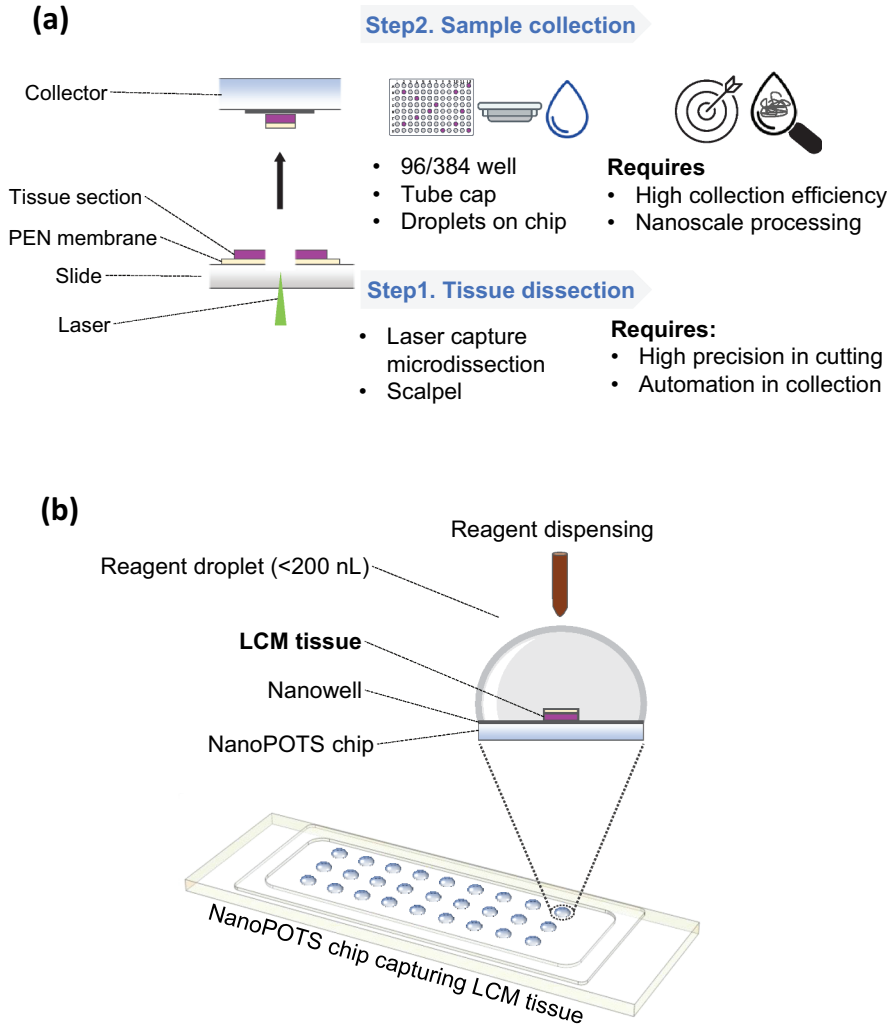

Figure 2. Tissue microdissection and nanoscale sample processing are key components of spatial proteomics. (a) step 1 centers on tissue dissection, typically performed using LCM, which allows precise isolation of targeted ROIs from tissue sections, ensuring accurate sampling of specific cellular populations. Step 2 highlights sample collection, where the isolated tissue is captured on various sample processing devices. (b) diagram for droplet-based dispensing and sample processing (e.g. reduction, alkylation, digestion) on each of the nanowell with LCM-dissected tissue section.

a hollow array of blades spaced hundreds of micrometers apart, allowing for tissue to be sliced into many micro fragments simultaneously by being pushed through the bladed array [29]. The μDicer has yet to be applied to spatial omics or proteomics profiling but might become a useful tool for achieving spatial proteomics with moderate resolution (e.g. ~200 μm). Tissue expansion is another interesting technique for enhancing manual tissue micro sampling by providing 160 μm lateral resolution without the need for special equipment [30]. This process involves reversible anchoring proteins into hydrogel polymer network within the biological tissue, allowing the specimen to be isotropically magnified.

Outside of these manual or mechanical approaches, LCM is the reigning method of choice for most spatial proteomics workflows. LCM precisely isolates ROIs on tissue sections by applying a laser while visualizing the tissue under a microscope [31,32]. LCM offers high precision and is particularly useful for isolating small or highly heterogeneous tissue regions. While LCM is a relatively mature technology, continuous advances in laser, microscopy, and automation contribute to the improvement in attainable precision and efficiency. A challenge for LCM in spatial proteomics has been the efficient and precise collection of near-single-cell samples for downstream processing and LC-MS analyses. Several techniques have been developed to enhance the efficiency of sample collection/processing for LCM-enabled spatial proteomics, such as the microfluidic based nanoPOTS (nanodroplet Processing in One-pot for Trace Samples) chip [33] which can be coupled to LCM to facilitate efficient sample collection with automatic sample transfer into nanodroplets [34]. The LCM-nanoPOTS platform employs hydrophilic reaction vessels for collection of LCM tissues into prepopulated DMSO droplets [34] and an optimized sample processing protocol to minimize surface-induced nonspecific protein adsorption [35]. More recently, a DUV-nanoPOTS (deep ultraviolet laser ablation microdissection combined with nanoPOTS) technique was reported for tissue dissection at cellular and subcellular resolution [36]. The implementation of a shorter wavelength UV laser enabled greater beam focusing and therefore improved spatial resolution. Another LCM-based technique referred to as 'Deep Visual Proteomics' has demonstrated the potential of integration of AI-driven image analysis with LCM for isolating tissue samples based on immunofluorescence imaging and machine learning based cell segmentation [25]. Such concepts provide a glimpse into the future direction of tissue dissection techniques that will not only allow for robust, precise, and automated tissue selection down to single cell levels, but also enable spatial proteomics at cellular resolution [25,37].

Unlike barcoding-based methods such as spatial transcriptomics (e.g. 10X Genomics Visium [12,38]), spatial proteomics relies on selection and precise tissue excision of ROIs based on high-resolution images. Once excised, the samples are processed for LC-MS analysis, with the resulting data linked back to the tissue image for spatial context. In this workflow, a critical need is to maintain reliable sample tracking throughout the process. Without barcoding, each sample must be assigned a unique identifier during LCM collection, which is tracked through every stage of sample processing and LC-MS analysis. Preserving the spatial context is also essential for downstream analyses. Capturing high-resolution images before and after tissue dissection helps document the exact tissue region being sampled. Integrating proteomics data with spatial metadata ensures that protein abundances can be mapped back to the original spatial location using bioinformatics tools (vide infra).

4. Nanoscale sample processing

The ability to process samples containing a very small amount of protein while minimizing sample loss is a critical element in spatial proteomics. Many techniques have been developed to address the potential sample loss for low-input samples. For example, the SISPROT (the simple and integrated proteomics sample preparation technology) was designed to couple LCM with a two-stage spintip device packed with C18 disk and strong cation exchange beads to ensure good sample recovery [39]. NanoPOTS represents one of the first technologies that enabled label-free proteomics from single cells or near-single-cell samples using a microfluidic sample preparation method [33]. NanoPOTS has been demonstrated to minimize surface adsorption of protein with the hanging-droplet technique [34,35] and drastically improve the overall recovery by performing all processing steps in nanoliter volumes (<200 nL). Several other methods have emerged to address the challenge of minimizing loss in low-input samples, including technologies like the integrated proteome analysis device (iPAD) [40], oil-air-droplet (OAD) [41], and the integrated proteomics chip (iProChip) [42]. Additionally, innovations such as automated processing in one pot for trace samples (autoPOTS) [43], surfactant-assisted one-pot (SOP) processing [44], water droplet-in-oil digestion (WinO) [45], and mass-adaptive coating-assisted single-cell proteomics (Mad-CASP) [46] have been developed, all of which build upon similar concepts to minimize surface adsorption loss. Several techniques have also been reported specifically for scProteomics processing. The nPOP technique uses a piezoelectric capillary (cellenONE instrument) to dispense individual cells in 300 picoliter droplets onto a fluorocarbon-coated glass slide before parallel processing of the cells through lysing, digestion, and isobaric labeling in volumes as low as 8–20 nl [47]. The proteoCHIP, an automated nanowell-array workflow, offers another universal solution for scProteomics, supporting multiplexed isobaric labeling of up to 16-plex with high sensitivity and throughput [48]. This system can be integrated with commercial platforms, like the cellenONE, for automated processing, combining single-cell dissociation with picoliter dispensing for downstream LC-MS analysis.

5. Sensitivity and throughput of LC-MS instrumentation

Both scProteomics and spatial proteomics require high sensitivity to achieve in-depth proteome coverage from limited samples and high analytical throughput of LC-MS platforms to analyze thousands of samples in a single study. Advances in LC separations, particularly robust ones with short gradients, are crucial for achieving high-throughput analyses [49]. For

example, the Evosep One and Vanquish Neo systems excel in delivering very short gradients (e.g. 1–10 min per run) while maintaining excellent chromatographic resolution, ideal for high-throughput needs in spatial and scProteomics. The Evosep One uses a split-flow system for rapid sample loading and elution, enhancing throughput by reducing the duty cycle [50]. This makes Evosep highly compatible with modern mass spectrometers featuring fast acquisition rates, such as the timsTOF or orbitrap Astral [51,52]. Similarly, the Vanquish Neo [53] offers flexible gradient times and flow rates, making it adaptable to diverse proteomics workflows.

With the fast acquisition rates of modern mass analyzers, LC separations with <10 min gradients can now be utilized to achieve deep proteome coverage for single cells or spatial proteomics, particularly when operated in data-independent acquisition (DIA) mode [54]. Recent advances in MS instrumentation have been pivotal in enabling this direction by providing the required sensitivity and speed for achieving comprehensive proteome coverage for limited samples. Exemplary systems include the Orbitrap [55] and timsTOF (trapped ion mobility spectrometry time-of-flight) [56] mass analyzers. The Orbitrap is renowned for its high resolution, mass accuracy, and dynamic range. Recent advances in Orbitrap analyzers, including higher-field Orbitraps and enhanced ion optics, advanced fragmentation techniques such as higher-energy C-trap dissociation (HCD), and signal processing have further improved the overall sensitivity, proteome coverage, and throughput of proteomic analyses [57–60]. In addition, high-field asymmetric waveform ion mobility spectrometry (FAIMS) is often incorporated as an interface with Orbitrap to effectively filter out singly charged ions and background ions [61]. scProteomics profiling has been demonstrated using a variety of Orbitrap platforms, including the Eclipse [42,62], Fusion Lumos [63], and Q-Exactive [44,64]. We have reported the Transferring Identification Based on FAIMS Filtering (TIFF) method that leverages FAIMS to extend ion accumulation times, which boosts MS sensitivity, thereby increasing peptide identification rates and quantification in single-cell proteomics [62,65]. These advancements further enabled deep spatial proteome mapping of the human pancreatic islet microenvironment with a lateral resolution of 50 µm, allowing the exploration of cellular heterogeneity and functional tissue unit-specific protein expression profiles [24]. The timsTOF mass analyzer combines ion mobility spectrometry (IMS) with time-of-flight (TOF) MS to achieve high sensitivity and rapid acquisition rates. IMS offers an additional dimension of separation, significantly enhancing coverage depth. The parallel accumulation-serial fragmentation (PASEF) technique [66,67] further enhances acquisition speed by allowing for simultaneous ion trapping, IMS separation, and TOF measurements. The Orbitrap Astral mass analyzer represents another significant recent advance toward high-throughput and high-sensitivity single cell or spatial proteomics analyses. This analyzer is notable for its nearly lossless ion transfer, high sensitivity, high resolution (80,000 at m/z 524) and accuracy at extraordinary acquisition speed (up to 200 hz when operated in DIA mode), making it particularly effective for low input samples [57,59].

Innovations in LC-MS/MS acquisition methods have also significantly enhanced the sensitivity, throughput, and data quality of proteomic analyses. Examples include: 1) the Boxcar acquisition method [68], which uses multiplexed m/z windows to improve low-abundance ion detection; 2) Synchronous Precursor Selection (SPS)-MS3 [69], which reduces co-isolation distortion and enhances quantitative accuracy; 3) Real-Time Searching (RTS) [70], enabling real-time identifications for better data acquisition efficiency; and 4) Speedy-PASEF [71], which combines dia-PASEF with fast chromatography to further boosts throughput, making it suitable for large-scale analyses.

6. Advances in bioinformatics tools for spatial proteomics

The merging of spatial proteomics necessitates the need of bioinformatics tools capable of incorporating, analyzing, and visualizing the additional spatial dimension of proteomic data. Notably, image co-registration is often required for aligning protein measurements with higher resolution IHC or immunofluorescent images. This alignment challenge has been well recognized in MS imaging (MSI) applications and several tools have been developed for alignment of images across modalities [72–74]. The bottom-up LC-MS/MS datasets acquired in a typical spatial proteomics workflow, however, have not been amenable for these image co-registration algorithms due to the larger pixel or voxel sizes (typically >40 µm) and different file formats relative to MSI studies. However, a universal framework for the integration of multimodal spatial omics datasets was introduced to address this challenge by allowing for shapes such as distinct polygonal ROIs (akin to those that are produced by LCM microscopes) to be defined spatially under a common coordinate system [75]. This Python-based framework, SpatialData, further allows for interoperability with existing multimodal analysis approaches such as Squidpy [76], Scanpy [77], and others [78]. Hence, protein abundances can now be plotted and visualized in the context of IF/IHC, spatial transcriptomics, or other multimodal images often collected as a part of a spatial multiomics study.

The additional spatial dimension in spatial proteomics will likely pose challenges for existing data repositories. Current repositories, such as PRIDE [79] and MassIVE [80], supports new analyses and machine learning models [81]. However, the unique nature of spatial or multimodal data introduces new complexities that existing repository architectures may not fully equipped to support. These challenges include the need for advanced storage solutions that can accommodate the spatial dimensions, along with robust tools for data integration and interpretation. While repositories like ProteomeXchange [79] are crucial for data sharing, they may become insufficient since they were originally designed for non-spatial data. Consequently, there is a growing demand for innovative bioinformatics tools and repository infrastructures capable of managing the complexities of spatial datasets. This includes enhanced metadata annotations, integration of spatial context, and the development of new algorithms for data processing and analysis. The HuBMAP consortium [6] is at the forefront of addressing these challenges by integrating diverse data types at the cellular level. Their data portal and reference atlas are designed to facilitate data reuse and improve

biological insights [82]. Initiatives like HarmonizR and the scProteomics R package represents excellent starting points toward dataset integration and promoting reproducible analysis across institutions and labs [83,84]. As spatial data becomes more prevalent, there will likely be a need for novel repository systems and analytical frameworks tailored to these complexities to ensure seamless data accessibility and utility.

7. Conclusion

Given the technological advances in tissue dissection, nanoscale sample processing, and LC-MS instrumentation, the field of spatial proteomics have made significant strides in demonstrating spatially resolved proteome profiling of heterogeneous tissue sections with (near) single-cell resolution, along with a significant coverage (e.g. >1000 proteins).

Table 1 summarizes selected studies of spatial proteomics over the past 5 years exemplifying diverse spatial resolution and proteome coverage. These studies showcase the potential of unbiased spatial proteome profiling in various tissues and biological contexts. While early studies offered only a moderate spatial resolution (>100 µm lateral resolution) [85,86], more recent studies have demonstrated successful tissue proteome mapping at the near-single-cell resolution [24] and even single-cell resolution [36,37] through the integration of high-resolution LCM, advanced nanoscale processing (e.g. nanoPOTS chips), and state-of-the art mass analyzers. Although these workflows still suffer from challenges in analytical throughput and overall proteome coverage, these studies illustrate the promise of MS-based spatial proteomics towards single-cell resolution. We anticipate that spatial proteomics will serve as an important complementary tool for other spatial omics technologies, helping to unravel new biological insights in (patho)physiology.

8. Expert opinion

We have witnessed major advances in spatially resolved proteome mapping on heterogeneous tissue sections with resolution at near-single-cell or single-cell levels. Spatial proteomics is becoming a valuable complement to molecular pathology and an enabling tool in spatial biology. However, major technological challenges persist, including the need for AI-assisted tissue dissection at high resolution and the requirement for high sensitivity and throughput of LC-MS platforms to fully realize the discovery power of spatial proteomics. Future developments in LC-MS instrumentation are perhaps the most easily anticipated, with expected enhancements in sensitivity, resolution, and analytical throughput. The new generation of timsTOF mass spectrometers have been recently demonstrated in scProteomics applications (e.g. timsToF SCP, timsTOF Ultra, and timsTOF Ultra 2). The combination of increased sensitivity, fast acquisition, modern DIA methods, along with advanced software suite will significantly enhance measurement throughput for label-free quantitation (LFQ) spatial proteomics [88]. Similarly, multiplexing approaches including isobaric (e.g. tandem mass tags, TMT) and non-isobaric (e.g. plexDIA [89], mDIA [90]) labeling will continue to enhance the sample throughput. For example, the latest iteration of TMT reagents has been expanded to allow for 32-plex with the capability to analyze up to 1,000 single-cells per day [91]. Novel hyperplexing strategies combining non-isobaric with isobaric labeling methods are on the horizon [91]. A well-recognized challenge of the multiplexing approach is compromised quantification accuracy [24] compared to label-free approaches. However, we anticipate that this limitation will be alleviated through further advancements in the resolution of MS instrumentation and bioinformatics.

More relevant to spatial biology will be developments in automated and intelligent tissue sampling techniques that enable precise and high-resolution dissection. Current tissue dissection method, such as LCM and MASP, have advanced the field of spatial biology, but they also face limitations. For example, in LCM, there is the potential for sample loss along the laser beam path, which is typically 2–5 µm in width. When using physical tools like steel blades, this can lead to reduced protein recovery and spatial resolution. In conventional LCM, the use of polymer membrane-coated slides introduces additional challenges, such as poor tissue adhesion, autofluorescence, low optical transparency, and reduced protein extraction efficiency. Furthermore, heat damage from the laser can compromise sample integrity and adversely impact downstream analyses. One example of high-resolution

Table 1. Selected spatial proteomics studies with a summary of their workflows and performance metrics.

Imaging Method	Tissue isolation method	Spatial resolution	LC-MS system	LC gradient	Protein identifications	Year, Ref.
H&E staining	Laser capture microdissection	100 µm	50 µm x 700 mm C18, Q Exactive Plus Orbitrap	97 min	2940 proteins	2020 [85],
Immunohistochemistry staining	Laser capture microdissection	5 mm^2	100 µm x 200 mm C18, Q Exactive HF-X	120 min	>660 Proteins	2020 [86],
Immunofluorescence staining	Laser capture microdissection	100–200 single cells	75 µm x 500 mm C18, timsTOF Plus	55 min	~5000 proteins	2022 [25],
Entire section	Micro-scaffold compartmentalization	400 µm	75 µm x 650 mm C18, Orbitrap Fusion Lumos	130 min	>5000 proteins	2022 [28],
H&E staining	Laser capture microdissection	7 µm	50 µm x 250 mm C18, Orbitrap Fusion Lumos	30 min	1312	2023 [36],
Immunofluorescence staining	Laser capture microdissection	Single shape	150 µm x 150 mm C18, timsTOF SCP	31 min	1712 proteins	2023 [37],
H&E staining	Laser capture microdissection	40 µm	75 µm x 150 mm C18, timsTOF Pro	17 min	1500 proteins	2023 [87],
H&E staining	Laser capture microdissection	50 µm	50 µm x 250 mm C18, Orbitrap Fusion Lumos	30 min	~3500 proteins	2024 [24],

dissection is LCM with UV lasers and infrared lasers [92]. Wavelengths with smaller beam widths and ablation-based methods will continue to improve achievable spatial resolution. Furthermore, higher-energy UV lasers can eliminate the dependence on specialized membrane slides that interfere with fluorescence microscopy. Alternatively, cryo-focused ion beam milling (Cryo-FIB) can potentially achieve ultra-high spatial resolution but has yet to be realized in the context of spatial proteomics. Cryo-FIB applies a beam (5–10 nm width) of ions (often gallium) to 'etch' or remove biological material within an ROI [93]. In a typical Cryo-FIB experiment, cryogenic lift-out is used to transfer or isolate an ROI for downstream Cryo-ET imaging. We envision the combination of Cryo-FIB with ultrasensitive proteomics can potentially open a new frontier in spatial biology at subcellular resolution. Finally, the implementation of machine learning methods will also help improve the precision and throughput of LCM by automating the selection of ROIs across tissue sections using available imaging information [25].

The concept of 3D spatial proteomics will soon become a reality through the combination of serial sectioning and spatial proteomics with the above outlined advances. This will enable the generation of 3D-spatial proteomic maps of tissues for thousands of proteins at cellular resolution. Heterogenous organs with complex structure and organization, such as mammalian brain, will greatly benefit from these technological advances, as will equivalently heterogenous tissues in other biological systems, like plant roots or microbial colonies. Advances in computational tools will facilitate reconstruction of the 3D maps from proteomics data across regions much larger than what is currently being measured. Additionally, a holistic, systems biology understanding of the spatial context will necessitate connecting single-cell and spatial proteomics to other -omes, such as the transcriptome, metabolome, or lipidome. Toward this goal, we have recently developed a novel approach for same-cell scProteomics and scRNAseq (nanoSPLITS), which has been demonstrated on dissociated cells but can be realistically extended to LCM tissue dissection for MS-enabled spatial multiomics at cellular resolution [94,95].

In the near term, the outlook for spatial proteomics is promising. The applications of spatial proteomics align well with the ongoing spatial atlas-focused consortia – such as HubMAP [6], HTAN [7], Kidney Precision Medicine Project [96]) – and will continue to play an important role in the shared goals of spatially characterizing tissues at cellular resolution in different contexts. We recognize that competing technologies will also drive necessary innovation in MS-based spatial proteomics. Next generation sequencing-based methods that incorporate oligo-labeled antibodies and spatial barcodes will continue to gain popularity due to their high commercialization potential, general compatibility with commercially available sequencers, and broad applicability to archived FFPE samples [11–14,18]. If nanopore-based sequencing of protein molecules can overcome current technical hurdles, it could also become a driving technology in spatial proteomics [97]. However, MS-based spatial proteomics is set to significantly impact biological discoveries, with expect rapid advancements in both technology and computational methods.

Funding

This work was supported by National Institutes of Health grants U54DK127823, R01DK135081, UH3CA256959, R01CA272377.

Declaration of interest

J.M.F is an inventor on a U.S. provisional patent application for the design of nanoSPLITS devices and associated operation methods (Application number: 63/250,011 filed 09/29/2021). The authors have no other relevant affiliations or financial involvement with any organization or entity with a financial interest in or financial conflict with the subject matter or materials discussed in the manuscript. This includes employment, consultancies, honoraria, stock ownership or options, expert testimony, grants or patents received or pending, or royalties.

Reviewer disclosures

Peer reviewers on this manuscript have no relevant financial or other relationships to disclose.

Author contributions

All authors made a significant contribution to the work reported. All authors reviewed and edited the drafts and approved the final version of the manuscript.

ORCID

Yumi Kwon http://orcid.org/0000-0003-0523-6197
James M. Fulcher http://orcid.org/0000-0001-9033-3623
Ljiljana Paša-Tolić http://orcid.org/0000-0001-9853-5457
Wei-Jun Qian http://orcid.org/0000-0002-5393-2827

References

Papers of special note have been highlighted as either of interest (•) or of considerable interest (••) to readers.

1. Mollgard K, Beinlich FRM, Kusk P, et al. A mesothelium divides the subarachnoid space into functional compartments. Science. 2023;379(6627):84–88. doi: 10.1126/science.adc8810
2. Huang JL, Pourhosseinzadeh MS, Lee S, et al. Paracrine signalling by pancreatic δ cells determines the glycaemic set point in mice. Nat Metab. 2024;6(1):61–77. doi: 10.1038/s42255-023-00944-2
3. Fu T, Dai LJ, Wu SY, et al. Spatial architecture of the immune microenvironment orchestrates tumor immunity and therapeutic response. J Hematol Oncol. 2021;14(1):98. doi: 10.1186/s13045-021-01103-4
4. Xue LY, Butler NJ, Makrigiorgos GM, et al. Bystander effect produced by radiolabeled tumor cells in vivo. Proc Natl Acad Sci U S A. 2002;99(21):13765–13770. doi: 10.1073/pnas.182209699
5. Nelson G, Wordsworth J, Wang C, et al. A senescent cell bystander effect: senescence-induced senescence. Aging Cell. 2012;11(2):345–349. doi: 10.1111/j.1474-9726.2012.00795.x
6. Hu BC, Lin S, Posgai A. The human body at cellular resolution: the NIH human biomolecular atlas program. Nature. 2019;574(7777):187–192. doi: 10.1038/s41586-019-1629-x
7. Rozenblatt-Rosen O, Regev A, Oberdoerffer P, et al. The human tumor atlas network: charting tumor transitions across space and time at single-cell resolution. Cell. 2020;181(2):236–249. doi: 10.1016/j.cell.2020.03.053
8. Lim J, Park C, Kim M, et al. Advances in single-cell omics and multiomics for high-resolution molecular profiling. Exp Mol Med. 2024;56(3):515–526. doi: 10.1038/s12276-024-01186-2
9. Bressan D, Battistoni G, Hannon GJ. The dawn of spatial omics. Science. 2023;381(6657):eabq4964. doi: 10.1126/science.abq4964

10. Chen KH, Boettiger AN, Moffitt JR, et al. RNA imaging. Spatially resolved, highly multiplexed RNA profiling in single cells. Science. 2015;348(6233):aaa6090. doi: 10.1126/science.aaa6090
11. Rodriques SG, Stickels RR, Goeva A, et al. Slide-seq: a scalable technology for measuring genome-wide expression at high spatial resolution. Science. 2019;363(6434):1463–1467. doi: 10.1126/science.aaw1219
12. Stahl PL, Salmen F, Vickovic S, et al. Visualization and analysis of gene expression in tissue sections by spatial transcriptomics. Science. 2016;353(6294):78–82. doi: 10.1126/science.aaf2403
13. Oliveira MF, Romero JP, Chung M, et al. Characterization of immune cell populations in the tumor microenvironment of colorectal cancer using high definition spatial profiling. bioRxiv. 2024 Jun 04:597233.
14. Wei X, Fu S, Li H, et al. Single-cell stereo-seq reveals induced progenitor cells involved in axolotl brain regeneration. Science. 2022;377(6610):eabp9444. doi: 10.1126/science.abp9444
15. Buchberger AR, DeLaney K, Johnson J, et al. Mass spectrometry imaging: a review of emerging advancements and future insights. Anal Chem. 2018;90(1):240–265. doi: 10.1021/acs.analchem.7b04733
16. Tian H, Sparvero LJ, Anthonymuthu TS, et al. Successive high-resolution (H2O)n-GCIB and C60-sims imaging integrates multi-omics in different cell types in breast cancer tissue. Anal Chem. 2021;93(23):8143–8151. doi: 10.1021/acs.analchem.0c05311
17. Yagnik G, Liu Z, Rothschild KJ, et al. Highly multiplexed immunohistochemical MALDI-MS imaging of biomarkers in tissues. J Am Soc Mass Spectrom. 2021;32(4):977–988. doi: 10.1021/jasms.0c00473
18. Liu Y, DiStasio M, Su G, et al. High-plex protein and whole transcriptome co-mapping at cellular resolution with spatial cite-seq. Nat Biotechnol. 2023;41(10):1405–1409. doi: 10.1038/s41587-023-01676-0
19. Giesen C, Wang HA, Schapiro D, et al. Highly multiplexed imaging of tumor tissues with subcellular resolution by mass cytometry. Nat Methods. 2014;11(4):417–422. doi: 10.1038/nmeth.2869
20. Black S, Phillips D, Hickey JW, et al. CODEX multiplexed tissue imaging with DNA-conjugated antibodies. Nat Protoc. 2021;16(8):3802–3835. doi: 10.1038/s41596-021-00556-8
21. Smith LM, Kelleher NL. Consortium for top down P. Proteoform: a single term describing protein complexity. Nat Methods. 2013;10(3):186–187. doi: 10.1038/nmeth.2369
22. Zemaitis KJ, Velickovic D, Kew W, et al. Enhanced spatial mapping of histone proteoforms in human kidney through MALDI-MSI by high-field UHMR-Orbitrap detection. Anal Chem. 2022;94(37):12604–12613. doi: 10.1021/acs.analchem.2c01034
23. Su P, McGee JP, Durbin KR, et al. Highly multiplexed, label-free proteoform imaging of tissues by individual ion mass spectrometry. Sci Adv. 2022;8(32):eabp9929. doi: 10.1126/sciadv.abp9929
24. Kwon Y, Woo J, Yu F, et al. Proteome-scale tissue mapping using mass spectrometry based on label-free and multiplexed workflows. Mol cell proteomics. 2024: 100841. Mol & Cellular Proteomics. 2024;23(11):100841. doi: 10.1016/j.mcpro.2024.100841

•• **Spatial proteomics at 50 µm for human islet microenvironment and head-to-head comparison of label-free and TMT quantification.**

25. Mund A, Coscia F, Kriston A, et al. Deep visual proteomics defines single-cell identity and heterogeneity. Nat Biotechnol. 2022;40(8):1231–1240. doi: 10.1038/s41587-022-01302-5

•• **The Deep Visual Proteomics concept where AI-driven image analysis with automated single-cell and single nucleus laser microdissection was introduced.**

26. Petyuk VA, Qian WJ, Chin MH, et al. Spatial mapping of protein abundances in the mouse brain by voxelation integrated with high-throughput liquid chromatography-mass spectrometry. Genome Res. 2007;17(3):328–336. doi: 10.1101/gr.5799207
27. Liu D, Smith DJ. Voxelation and gene expression tomography for the acquisition of 3-D gene expression maps in the brain. Methods. 2003;31(4):317–325. doi: 10.1016/S1046-2023(03)00162-2
28. Ma M, Huo S, Zhang M, et al. In-depth mapping of protein localizations in whole tissue by micro-scaffold assisted spatial proteomics (MASP). Nat Commun. 2022;13(1):7736. doi: 10.1038/s41467-022-35367-2
29. Cordts SC, Castaño N, Koppaka S, et al. Fabrication of a silicon µDicer for uniform microdissection of tissue samples. Appl Phys Lett. 2021;119(1). doi: 10.1063/5.0053792
30. Li L, Sun C, Sun Y, et al. Spatially resolved proteomics via tissue expansion. Nat Commun. 2022;13(1):7242. doi: 10.1038/s41467-022-34824-2
31. Longuespee R, Alberts D, Pottier C, et al. A laser microdissection-based workflow for FFPE tissue microproteomics: important considerations for small sample processing. Methods. 2016;104:154–162. doi: 10.1016/j.ymeth.2015.12.008
32. Espina V, Wulfkuhle JD, Calvert VS, et al. Laser-capture microdissection. Nat Protoc. 2006;1(2):586–603. doi: 10.1038/nprot.2006.85
33. Zhu Y, Piehowski PD, Zhao R, et al. Nanodroplet processing platform for deep and quantitative proteome profiling of 10–100 mammalian cells. Nat Commun. 2018;9(1):882. doi: 10.1038/s41467-018-03367-w
34. Zhu Y, Dou M, Piehowski PD, et al. Spatially resolved proteome mapping of laser capture microdissected tissue with automated sample transfer to Nanodroplets. Mol Cell Proteomics. 2018;17(9):1864–1874. doi: 10.1074/mcp.TIR118.000686
35. Kwon Y, Piehowski PD, Zhao R, et al. Hanging drop sample preparation improves sensitivity of spatial proteomics. Lab Chip. 2022;22(15):2869–2877. doi: 10.1039/D2LC00384H
36. Xiang P, Liyu A, Kwon Y, et al. Spatial proteomics toward subcellular resolution by coupling deep ultraviolet laser ablation with nanodroplet sample preparation. ACS Meas Sci Au. 2023;3(6):459–468. doi: 10.1021/acsmeasuresciau.3c00033
37. Rosenberger FA, Thielert M, Strauss MT, et al. Spatial single-cell mass spectrometry defines zonation of the hepatocyte proteome. Nat Methods. 2023;20(10):1530–1536. doi: 10.1038/s41592-023-02007-6

•• **The first demonstration of spatial proteomics at the single cell resolution with the AI-driven cell segmentation and laser microdissection.**

38. Salmen F, Stahl PL, Mollbrink A, et al. Barcoded solid-phase RNA capture for spatial Transcriptomics profiling in mammalian tissue sections. Nat Protoc. 2018;13(11):2501–2534. doi: 10.1038/s41596-018-0045-2
39. Xu R, Tang J, Deng Q, et al. Spatial-resolution cell type proteome profiling of cancer tissue by fully integrated proteomics technology. Anal Chem. 2018;90(9):5879–5886. doi: 10.1021/acs.analchem.8b00596
40. Shao X, Wang XT, Guan S, et al. Integrated proteome analysis device for fast single-cell protein profiling. Anal Chem. 2018;90(23):14003–14010. doi: 10.1021/acs.analchem.8b03692
41. Li ZY, Huang M, Wang XK, et al. Nanoliter-scale oil-Air-droplet Chip-based single cell Proteomic analysis. Anal Chem. 2018;90(8):5430–5438. doi: 10.1021/acs.analchem.8b00661
42. Gebreyesus ST, Siyal AA, Kitata RB, et al. Streamlined single-cell proteomics by an integrated microfluidic chip and data-independent acquisition mass spectrometry. Nat Commun. 2022;13(1):37. doi: 10.1038/s41467-021-27778-4
43. Liang YR, Acor H, McCown MA, et al. Fully automated sample processing and analysis workflow for low-input proteome profiling. Anal Chem. 2021;93(3):1658–1666. doi: 10.1021/acs.analchem.0c04240
44. Tsai CF, Zhang P, Scholten D, et al. Surfactant-assisted one-pot sample preparation for label-free single-cell proteomics. Commun Biol. 2021;4(1):265. doi: 10.1038/s42003-021-01797-9
45. Masuda T, Inamori Y, Furukawa A, et al. Water droplet-in-oil digestion method for single-cell proteomics. Anal Chem. 2022;94(29):10329–10336. doi: 10.1021/acs.analchem.1c05487
46. Li S, Su K, Zhuang Z, et al. A simple, rapid, and practical method for single-cell proteomics based on mass-adaptive coating of synthetic

peptides. Sci Bull. 2022;67(6):581–584. doi: 10.1016/j.scib.2021.12.022
47. Leduc A, Huffman RG, Cantlon J, et al. Exploring functional protein covariation across single cells using nPOP. Genome Biol. 2022;23(1):261. doi: 10.1186/s13059-022-02817-5
48. Ctortecka C, Hartlmayr D, Seth A, et al. An automated nanowell-array workflow for quantitative multiplexed single-cell proteomics sample preparation at high sensitivity. Mol Cell Proteomics. 2023;22(12):100665. doi: 10.1016/j.mcpro.2023.100665
49. Matzinger M, Mayer RL, Mechtler K. Label-free single cell proteomics utilizing ultrafast LC and MS instrumentation: a valuable complementary technique to multiplexing. Proteomics. 2023;23(13–14):e2200162. doi: 10.1002/pmic.202200162
50. Bache N, Geyer PE, Bekker-Jensen DB, et al. A novel LC system embeds analytes in pre-formed gradients for rapid, ultra-robust proteomics. Mol Cell Proteomics. 2018;17(11):2284–2296. doi: 10.1074/mcp.TIR118.000853
51. Krieger JR, Wybenga-Groot LE, Tong J, et al. Evosep one enables robust deep Proteome coverage using tandem Mass tags while significantly reducing instrument time. J Proteome Res. 2019;18(5):2346–2353. doi: 10.1021/acs.jproteome.9b00082
52. Viode A, van Zalm P, Smolen KK, et al. A simple, time- and cost-effective, high-throughput depletion strategy for deep plasma proteomics. Sci Adv. 2023;9(13):eadf9717. doi: 10.1126/sciadv.adf9717
53. Bian Y, Zheng R, Bayer FP, et al. Robust, reproducible and quantitative analysis of thousands of proteomes by micro-flow LC–MS/MS. Nat Commun. 2020;11(1):157. doi: 10.1038/s41467-019-13973-x
54. Heil LR, Damoc E, Arrey TN, et al. Evaluating the performance of the astral Mass analyzer for quantitative proteomics using data-independent acquisition. J Proteome Res. 2023;22(10):3290–3300. doi: 10.1021/acs.jproteome.3c00357
55. Zubarev RA, Makarov A. Orbitrap mass spectrometry. Anal Chem. 2013;85(11):5288–5296. doi: 10.1021/ac4001223
56. Fernandez-Lima F, Kaplan DA, Suetering J, et al. Gas-phase separation using a trapped ion mobility spectrometer. Int J Ion Mobil Spec. 2011;14(2–3):93–98. doi: 10.1007/s12127-011-0067-8
57. Petrosius V, Aragon-Fernandez P, Arrey TN, et al. Evaluating the capabilities of the astral mass analyzer for single-cell proteomics. bioRxiv. 2023 Jun 06:543943.
58. Guzman UH, Martinez-Val A, Ye Z, et al. Ultra-fast label-free quantification and comprehensive proteome coverage with narrow-window data-independent acquisition. Nat Biotechnol. 2024;42(12):1855–1866. doi: 10.1038/s41587-023-02099-7
59. Stewart HI, Grinfeld D, Giannakopulos A, et al. Parallelized acquisition of orbitrap and astral analyzers enables high-throughput quantitative analysis. Anal Chem. 2023;95(42):15656–15664. doi: 10.1021/acs.analchem.3c02856
60. Bekker-Jensen DB, Martínez-Val A, Steigerwald S, et al. A compact quadrupole-orbitrap Mass spectrometer with FAIMS interface improves proteome coverage in short LC gradients. Mol Cell Proteom Mcp. 2020;19(4):716–729. doi: 10.1074/mcp.TIR119.001906
61. Hebert AS, Prasad S, Belford MW, et al. Comprehensive single-shot proteomics with FAIMS on a hybrid Orbitrap Mass spectrometer. Anal Chem. 2018;90(15):9529–9537. doi: 10.1021/acs.analchem.8b02233
62. Cong YZ, Motamedchaboki K, Misal SA, et al. Ultrasensitive single-cell proteomics workflow identifies >1000 protein groups per mammalian cell. Chem Sci. 2021;12(3):1001–1006. doi: 10.1039/D0SC03636F
63. Williams SM, Liyu AV, Tsai CF, et al. Automated coupling of nanodroplet sample preparation with liquid chromatography–Mass spectrometry for high-throughput single-cell proteomics. Anal Chem. 2020;92(15):10588–10596. doi: 10.1021/acs.analchem.0c01551
64. Specht H, Emmott E, Petelski AA, et al. Single-cell proteomic and transcriptomic analysis of macrophage heterogeneity using SCoPE2. Genome Biol. 2021;22(1):50. doi: 10.1186/s13059-021-02267-5
65. Woo J, Clair GC, Williams SM, et al. Three-dimensional feature matching improves coverage for single-cell proteomics based on ion mobility filtering. Cell Syst. 2022;13(5):426–434. doi: 10.1016/j.cels.2022.02.003
66. Meier F, Brunner AD, Koch S, et al. Online parallel accumulation–serial fragmentation (PASEF) with a novel trapped ion mobility Mass spectrometer. Mol Cell Proteomics. 2018;17(12):2534–2545. doi: 10.1074/mcp.TIR118.000900
67. Meier F, Brunner AD, Frank M, et al. diaPASEF: parallel accumulation–serial fragmentation combined with data-independent acquisition. Nat Methods. 2020;17(12):1229–1236. doi: 10.1038/s41592-020-00998-0
68. Meier F, Geyer PE, Virreira Winter S, et al. BoxCar acquisition method enables single-shot proteomics at a depth of 10,000 proteins in 100 minutes. Nat Methods. 2018;15(6):440–448. doi: 10.1038/s41592-018-0003-5
69. McAlister GC, Nusinow DP, Jedrychowski MP, et al. MultiNotch MS3 enables accurate, sensitive, and multiplexed detection of differential expression across cancer cell line proteomes. Anal Chem. 2014;86(14):7150–7158. doi: 10.1021/ac502040v
70. Erickson BK, Mintseris J, Schweppe DK, et al. Active instrument engagement combined with a real-time database search for improved performance of sample multiplexing workflows. J Proteome Res. 2019;18(3):1299–1306. doi: 10.1021/acs.jproteome.8b00899
71. Szyrwiel L, Gille C, Mülleder M, et al. Speedy-pasef: analytical flow rate chromatography and trapped ion mobility for deep high-throughput proteomics. bioRxiv. 2023:02.17.528968.
72. Patterson NH, Yang E, Kranjec EA, et al. Co-registration and analysis of multiple imaging mass spectrometry datasets targeting different analytes. Bioinformatics. 2019;35(7):1261–1262. doi: 10.1093/bioinformatics/bty780
73. Balluff B, Heeren RMA, Race AM. An overview of image registration for aligning mass spectrometry imaging with clinically relevant imaging modalities. J Mass Spectrom Adv Clin Lab. 2022;23:26–38. doi: 10.1016/j.jmsacl.2021.12.006
74. Nikitina A, Huang D, Li L, et al. A Co-registration pipeline for multimodal MALDI and Confocal imaging analysis of stem cell colonies. J Am Soc Mass Spectrom. 2020;31(4):986–989. doi: 10.1021/jasms.9b00094
75. Marconato L, Palla G, Yamauchi KA, et al. SpatialData: an open and universal data framework for spatial omics. Nat Methods. 2024. doi: 10.1038/s41592-024-02212-x
76. Palla G, Spitzer H, Klein M, et al. Squidpy: a scalable framework for spatial omics analysis. Nat Methods. 2022;19(2):171–178. doi: 10.1038/s41592-021-01358-2
77. Wolf FA, Angerer P, Theis FJ. SCANPY: large-scale single-cell gene expression data analysis. Genome Biol. 2018;19(1):15. doi: 10.1186/s13059-017-1382-0
78. Gayoso A, Lopez R, Xing G, et al. A python library for probabilistic analysis of single-cell omics data. Nat Biotechnol. 2022;40(2):163–166. doi: 10.1038/s41587-021-01206-w
79. Perez-Riverol Y, Bai J, Bandla C, et al. The PRIDE database resources in 2022: a hub for mass spectrometry-based proteomics evidences. Nucleic Acids Res. 2022;50(D1):D543–D552. doi: 10.1093/nar/gkab1038
80. Choi M, Carver J, Chiva C, et al. MassIVE.Quant: a community resource of quantitative mass spectrometry–based proteomics datasets. Nat Methods. 2020;17(10):981–984. doi: 10.1038/s41592-020-0955-0
81. Beck AG, Muhoberac M, Randolph CE, et al. Recent developments in machine learning for Mass spectrometry. ACS Meas Sci Au. 2024;4(3):233–246. doi: 10.1021/acsmeasuresciau.3c00060
82. Borner K, Teichmann SA, Quardokus EM, et al. Anatomical structures, cell types and biomarkers of the human reference atlas. Nat Cell Biol. 2021;23(11):1117–1128. doi: 10.1038/s41556-021-00788-6
83. Vanderaa C, Gatto L. The current state of single-cell proteomics data analysis. Curr Protoc. 2023;3(1):e658. doi: 10.1002/cpz1.658
84. Voss H, Schlumbohm S, Barwikowski P, et al. HarmonizR enables data harmonization across independent proteomic datasets with

appropriate handling of missing values. Nat Commun. 2022;13 (1):3523. doi: 10.1038/s41467-022-31007-x

85. Piehowski PD, Zhu Y, Bramer LM, et al. Automated mass spectrometry imaging of over 2000 proteins from tissue sections at 100-μm spatial resolution. Nat Commun. 2020;11(1):8. doi: 10.1038/s41467-019-13858-z
    - **Demonstrated an efficient integration of LCM with the nanodroplet-based sample processing platform (nanoPOTS) for achieving 100 μm resolution in spatial proteomics.**
86. Huang P, Kong Q, Gao W, et al. Spatial proteome profiling by immunohistochemistry-based laser capture microdissection and data-independent acquisition proteomics. Anal Chim Acta. 2020;1127:140–148. doi: 10.1016/j.aca.2020.06.049
87. Davis S, Scott C, Oetjen J, et al. Deep topographic proteomics of a human brain tumour. Nat Commun. 2023;14(1):7710. doi: 10.1038/s41467-023-43520-8
88. Phlairaharn T, Ye Z, Krismer E, et al. Optimizing linear ion-trap data-independent acquisition toward single-cell proteomics. Anal Chem. 2023;95(26):9881–9891. doi: 10.1021/acs.analchem.3c00842
89. Derks J, Leduc A, Wallmann G, et al. Increasing the throughput of sensitive proteomics by plexDIA. Nat Biotechnol. 2023;41(1):50–59. doi: 10.1038/s41587-022-01389-w
90. Thielert M, Itang EC, Ammar C, et al. Robust dimethyl-based multiplex-dia doubles single-cell proteome depth via a reference channel. Mol Syst Biol. 2023;19(9):e11503. doi: 10.15252/msb.202211503
91. Leduc A, Khoury L, Cantlon J, et al. Massively parallel sample preparation for multiplexed single-cell proteomics using nPOP. Nat Protoc. 2024;19(12):3750–3776. doi: 10.1038/s41596-024-01033-8
92. Lawal RO, Richardson LT, Dong C, et al. Deep-ultraviolet laser ablation sampling for proteomic analysis of tissue. Anal Chim Acta. 2021;1184:339021. doi: 10.1016/j.aca.2021.339021
93. Lam V, Villa E. Practical approaches for cryo-fib milling and applications for cellular cryo-electron tomography. Methods Mol Biol. 2021;2215:49–82.
94. Kumar R, Zemaitis KJ, Fulcher JM, et al. Advances in mass spectrometry-enabled multiomics at single-cell resolution. Curr Opin Biotechnol. 2024;87:103096. doi: 10.1016/j.copbio.2024.103096
95. Fulcher JM, Markillie LM, Mitchell HD, et al. Parallel measurement of transcriptomes and proteomes from same single cells using nanodroplet splitting. Nat Commun. 2024;15(1):10614. doi: 10.1038/s41467-024-54099-z
96. Lake BB, Menon R, Winfree S, et al. An atlas of healthy and injured cell states and niches in the human kidney. Nature. 2023;619 (7970):585–594. doi: 10.1038/s41586-023-05769-3
97. Dorey A, Howorka S. Nanopore DNA sequencing technologies and their applications towards single-molecule proteomics. Nat Chem. 2024;16(3):314–334. doi: 10.1038/s41557-023-01322-x

Connective Tissue Research

ISSN: 0300-8207 (Print) 1607-8438 (Online) Journal homepage: www.tandfonline.com/journals/icts20

Spatial transcriptomic applications in orthopedics

Thomas L. Jenkins, Jasper H.N. Yik & Dominik R. Haudenschild

To cite this article: Thomas L. Jenkins, Jasper H.N. Yik & Dominik R. Haudenschild (10 May 2025): Spatial transcriptomic applications in orthopedics, Connective Tissue Research, DOI: 10.1080/03008207.2025.2501703

To link to this article: https://doi.org/10.1080/03008207.2025.2501703

Published online: 10 May 2025.

CONNECTIVE TISSUE RESEARCH
https://doi.org/10.1080/03008207.2025.2501703

Taylor & Francis
Taylor & Francis Group

Spatial transcriptomic applications in orthopedics

Thomas L. Jenkins [a], Jasper H.N. Yik [a], and Dominik R. Haudenschild [a,b]

[a]Department of Translational Orthopedic Research, Houston Methodist Research Institute, Houston, TX, USA; [b]Orthopedics & Sports Medicine, Houston Methodist Hospital, Houston, TX, USA

ABSTRACT

Purpose: This review highlights the transformative impact of spatial transcriptomics on orthopedic research, focusing on its application in deciphering intricate gene expression patterns within musculoskeletal tissues.

Methods: The paper reviews literature for spatial transcriptomic methods, specifically 10X Visium, 10X Xenium, seqFISH+, MERFISH, NanoString GeoMx DSP, used on musculoskeletal tissues (cartilage, joints, bone, tendon, ligament, and synovium).

Results: Searches identified 29 published manuscripts reporting spatial transcriptomic data in cartilage, bone, tendon, synovium, and intervertebral disc. Most publications of spatial transcriptomic data are from tendon and synovium. 10X Visium has been used in 22 of the 29 papers identified. Spatial transcriptomics has been used to identify novel cell populations and cell signaling pathways that regulate development and disease.

Conclusions: Imaging-based spatial transcriptomic methods may be better for hypothesis testing as they generally have subcellular resolution but sequence fewer genes. Sequencing methods may be better for untargeted, shotgun approaches that can generate useful hypotheses from the spatial data from unimpaired tissue sections. Spatial transcriptomic methods could become useful for clinical diagnostics and precision medicine approaches.

ARTICLE HISTORY
Received 3 July 2024
Accepted 29 April 2025

KEYWORDS
Spatial transcriptomics; cartilage; orthopedics; arthritis; synovium

Introduction

Musculoskeletal disorders are among the most common diseases and leading causes of disability in the world, affecting an estimated 1.7 billion people[1,2]. The prevalence of musculoskeletal disorders increased by 62% from 1990 to 2019[1]. Musculoskeletal disorders include osteoarthritis (OA), fractures, back injuries, tendon/ligament injuries, and rheumatoid arthritis (RA). More than 344 million people in the world suffer from OA[1], and the numbers are projected to affect nearly 1 billion people worldwide by 2050[3]. OA is a whole-joint disease characterized by cartilage degradation, subchondral bone remodeling, meniscal degeneration, and synovial inflammation that causes pain and disability[4–6]. Techniques employed to preserve the joint include physiological management (physical therapy, weight loss, exercise, braces), pharmacological intervention (steroids, hyaluronic acid injections), orthobiologics (platelet-rich plasma, stromal vascular fraction, stem cells), and operative methods (microfracture, subchondral drilling, osteochondral grafting, cell therapy)[7]. A common theme to many of these musculoskeletal disorders is a drastic change in cell organization after injury—one that often fails to regenerate the damaged tissues. A better understanding of the cell populations regulating musculoskeletal disorders could lead to more effective treatments and therapies to reduce the burden of musculoskeletal diseases.

Single-cell RNA-Seq (scRNA-Seq) can identify pathogenic cell populations and the cell populations regulating cell–cell and cell–tissue crosstalk during disease initiation and progression[8–10]. scRNA-Seq reveals cellular heterogeneity and discovers subclusters of cell populations, while also determining cell differentiation trajectories and cell signaling networks[9,11]. scRNA-Seq has revealed the cellular heterogeneity in OA and RA, identifying dozens of subtypes of chondrocytes, fibroblasts, and immune cells that regulate disease progression and homeostasis (summarized in[9,12]. scRNA-Seq analysis of healthy and diseased tendons has revealed at least 5 distinct types of tendon fibroblasts, in addition to epithelial cells, endothelial cells, T-cells, monocytes, and pericytes[13,14] – much more heterogeneity than previously thought[15,16]. However, scRNA-Seq has limitations. scRNA-Seq methods can require special dissociation protocols to collect the single cells before

CONTACT Dominik R. Haudenschild drhaudenschild@houstonmethodist.org Department of Translational Orthopedic Research, Houston Methodist Research Institute, 6770 Bertner Ave, Houston, TX USA 77030

Table 1. Comparison of spatial transcriptomic methods.

Type	Method	Commercial option	Spatial resolution	Number of genes
In Situ Capture	ST[18]	Visium (10X Genomics)	Multicellular (55 µm)	Whole Genome
		Visium HD (10X Genomics)	Single Cell (2 µm)	18,000+ (GP)
	Stereo-seq[19]	STOmics	Subcellular (500 nm)	Whole Genome
ROI Selection	GeoMx DSP[20]	NanoString	Single Cell (10 µm)	18,000+ (GP)
smFISH	smFISH[21,22,37]		Subcellular	4 (probes)
	seqFISH+[43]		Subcellular	65,536 (probes)
	MERFISH[23]	MERSCOPE (Vizgen)	Subcellular	10,000 (probes)
In Situ Sequencing	In Situ Sequencing[24]	Xenium (10X Genomics)	Subcellular	100–1000 (probes)

Abbreviations: DSP = digital spatial profiling; GP = gene panel; LCM = laser capture microdissection; MERFISH = multiplex error-robust fluorescent in situ hybridization; ROI = region-of-interest; smFISH = single-molecule fluorescent in situ hybridization; ST = spatial transcriptomics.

sequencing the transcriptome, which can cause difficulties for dense musculoskeletal tissues[9], and lose spatial information as they cannot be performed *in situ*.

Spatial transcriptomic methods allow *in situ* gene expression analysis without inducing stress, cell death, or cell aggregation into the system. Spatial transcriptomics captures mRNA from cells with known locations to enable the mapping of gene expression patterns and assigning cell types within intact tissue samples[17]. By visualizing gene expression patterns within tissues, researchers can gain a deeper understanding of how cells function in their native environments and how alterations in gene expression contribute to disease states. Advancements in spatial transcriptomics have given rise to a diverse array of techniques (Table 1), each with its unique strengths and applications. There are five main categories of spatial transcriptomic methods: 1) in situ capture with next-generation sequencing (NGS) methods and spatial barcoding, 2) in situ sequencing (ISS), 3) region-of-interest (ROI) selection, 4) single-molecule fluorescent in situ hybridization (smFISH), and 5) methods that do not require a priori spatial locations (e.g., in silico reconstruction[25,26] and DistMap[27,28], which will not be covered in this review[17]. While laser-capture microdissection followed by RNA-Seq can be considered an ROI selection spatial transcriptomic method, it will be omitted from this review as it physically destroys the tissue[17,29–36].

Methods

Searches for original research articles using spatial transcriptomics methods in musculoskeletal tissues were performed in PubMed (3 March 2025) with combinations of the musculoskeletal tissue terms ("Cartilage"[Mesh], "Joints"[Mesh], "Tendons"[Mesh], "Bone and Bones"[Mesh], "Synovial Membrane"[Mesh], "Ligament"[Mesh]) and spatial transcriptomics terms ("spatial transcriptomics," "Visium," "Xenium," "MERSCOPE," "MERFISH," "Vizgen," "GeoMx DSP," "Stereo-seq"). Additional searches occurred on the 10X Genomics publication list (https://www.10xgenomics.com/publications.; filters: "Spatial Gene Expression for Fresh Frozen," "Spatial Gene Expression for FFPE," "In Situ Gene Expression"), NanoString publication list (https://nanostring.com/resources/publications/.; categories: "GeoMx," "GeoMx DSP," "GeoMx—Digital Spatial Profiling"); and Vizgen publications list (https://vizgen.com/resources/publications/) with tissue terms (cartilage, synovium, joints, bone, tendon, ligament, meniscus). The inclusion of studies for review was any peer-reviewed original research paper that used a spatial transcriptomics method on a musculoskeletal tissue (Figure 1).

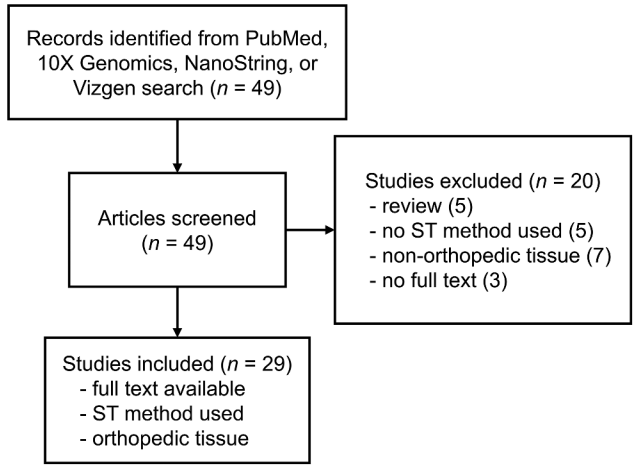

Figure 1. Flow diagram of search process and study inclusion and exclusion. Abbreviations: ST = spatial transcriptomics.

Results

Searching PubMed for "spatial transcriptomics" returned 9143 results (3 March 2025), with more than half reported between 2022 and 2025. Searches including musculoskeletal tissue terms on PubMed, 10X Genomics, NanoString, and Vizgen identified 49 articles for screening (Figure 1). After screening, 29 articles were included that had full text available using at least one spatial transcriptomic method on

Table 2. Summary of spatial transcriptomics methods used on musculoskeletal tissues. Empty cells were not reported in the text.

Spatial transcriptomics type	Spatial transcriptomics method	Tissue	Tissue preparation	Fixation	Section thickness (μm)	Permeabilization time (min)	Species	Ref:
In Situ Capture	10X Visium	Bone	Flash Frozen, OCT Embedded	Methanol	12	21	Mice	[38]
In Situ Capture	10X Visium	Bone	FFPE decalcified in 12.5% EDTA (pH 7.5) for 10 days at 4°C	10% NBF	5		Mice	[39]
In Situ Capture	10X Visium	Bone	FFPE Decalcification was performed with 10% EDTA (pH 7.2–7.4) for 2 weeks	4% PFA	5		Mice	[40]
In Situ Capture	10X Visium	Bone	FFPE 0.5 M pH 8 EDTA for 2 weeks	10% NBF	5		Mice	[41]
In Situ Capture	10X Visium	Cartilage Bone	FFPE decalcified with Formic Acid Bone Decalcifier for 16 hours at 4°C	10% NBF	5		Mice	[42]
In Situ Capture	10X Visium	Intrafratellar Fat Pad	Flash Frozen, OCT Embedded	Methanol			Human	[43]
In Situ Capture	10X Visium	Ligament					Human	[44]
In Situ Capture	10X Visium	Nucleus Pulposis	Flash Frozen, OCT Embedded		10		Mice	[45]
In Situ Capture	10X Visium	Synovium	Flash Frozen, OCT Embedded	2% NBF	7	20	Human	[46]
In Situ Capture	10X Visium	Synovium	Flash Frozen, OCT Embedded		10	12	Human	[47]
In Situ Capture	10X Visium	Synovium		Methanol	7	15	Human	[48]
In Situ Capture	10X Visium	Synovium					Human	[49]
In Situ Capture	10X Visium	Synovium		2% FA	7	20	Human	[50]
In Situ Capture	10X Visium	Synovium	Flash Frozen, OCT Embedded			15	Human	[51]
In Situ Capture	10X Visium	Tendon	Flash Frozen, OCT Embedded		10	10	Human	[52]
In Situ Capture	10X Visium	Tendon	Flash Frozen, OCT Embedded	Methanol	14	21	Rats	[53]
In Situ Capture	10X Visium	Tendon	Flash Frozen, OCT Embedded		10		Mice	[54]
In Situ Capture	10X Visium	Tendon					Human	[55]
In Situ Capture	10X Visium	Tendon	Flash Frozen, OCT Embedded		10		Human	[56]
In Situ Capture	10X Visium (Published Dataset)	Tendon						[57]
In Situ Capture	RNA-Rescue Spatial Transcriptomics	Cartilage	Flash Frozen, OCT Embedded	Formalin; 4% methanol	10		Mice	[58]
In Situ Capture	Stereo-Seq	Engineered Cartilage; Cartilage					Rats	[59]
In Situ Capture	Stereo-Seq	Enthesis	Flash Frozen, OCT Embedded	Methanol	10		Mice	[60]
In Situ Capture	Stereo-Seq	Whole Embryo; Bone; Cartilage; Connective Tissue; Mesenchyme	Flash Frozen, OCT Embedded	Methanol	10		Mice	[19]
In Situ Capture	10X Visium	Spine	Flash Frozen, OCT Embedded	3.7% FA		12	Human	[61]
In Situ Sequencing	10X Xenium							
In Situ Capture; In Situ Sequencing	10X Visium; In situ sequencing	Nucleus Pulposis	Flash Frozen, OCT Embedded				Mice	[62]
In Situ Sequencing; In Situ Capture	10X Xenium (CARTANA); 10X Visium	Shoulder; Hip; Knee; Cranium	Flash Frozen, OCT Embedded		10		Human	[63]
ROI Selection	GeoMx DSP	Synovium	Formalin Fixed, Paraffin Embedded	Formalin			Human	[64]
smFISH	smFISH	Engineered Cartilage		4% PFA			Bovine	[65]

Abbreviations: ACL = anterior cruciate ligament; E11.5–12.5 = embryonic stage; EDTA = ethylenediaminetetraacetic acid; FA = formaldehyde; FFPE = formalin fixed, paraffin-embedded; MSC = mesenchymal stem/stromal cell; NBF = neutrally buffered formalin; OCT = optimal cutting temperature medium; PFA = paraformaldehyde; ROI = region of interest; smFISH = single molecule fluorescent in situ hybridization.

a musculoskeletal tissue (Table 2). Papers were excluded on the following criteria: 1) review paper (5), 2) no spatial transcriptomic method used (5), 3) not applied to musculoskeletal tissue (i.e., nerve or cancer tissue) (7), or 4) unable to obtain free text (3). Of the spatial transcriptomics methods used, in situ capture has been primarily used (22 papers reporting 10X Visium spatial transcriptomics, 3 reporting Stereo-Seq), along with ROI selection methods, in situ sequencing methods, and single-molecule in situ hybridization-based methods (Table 2). Tendon, synovium, and bone are the musculoskeletal tissues with the most spatial transcriptomic data reported, but cartilage, intervertebral disc, intrafratellar fat pad, and whole joints have also been analyzed. An overview schematic of the techniques discussed in this review is shown in Figure 2. Examples of data obtained from the techniques discussed in this review

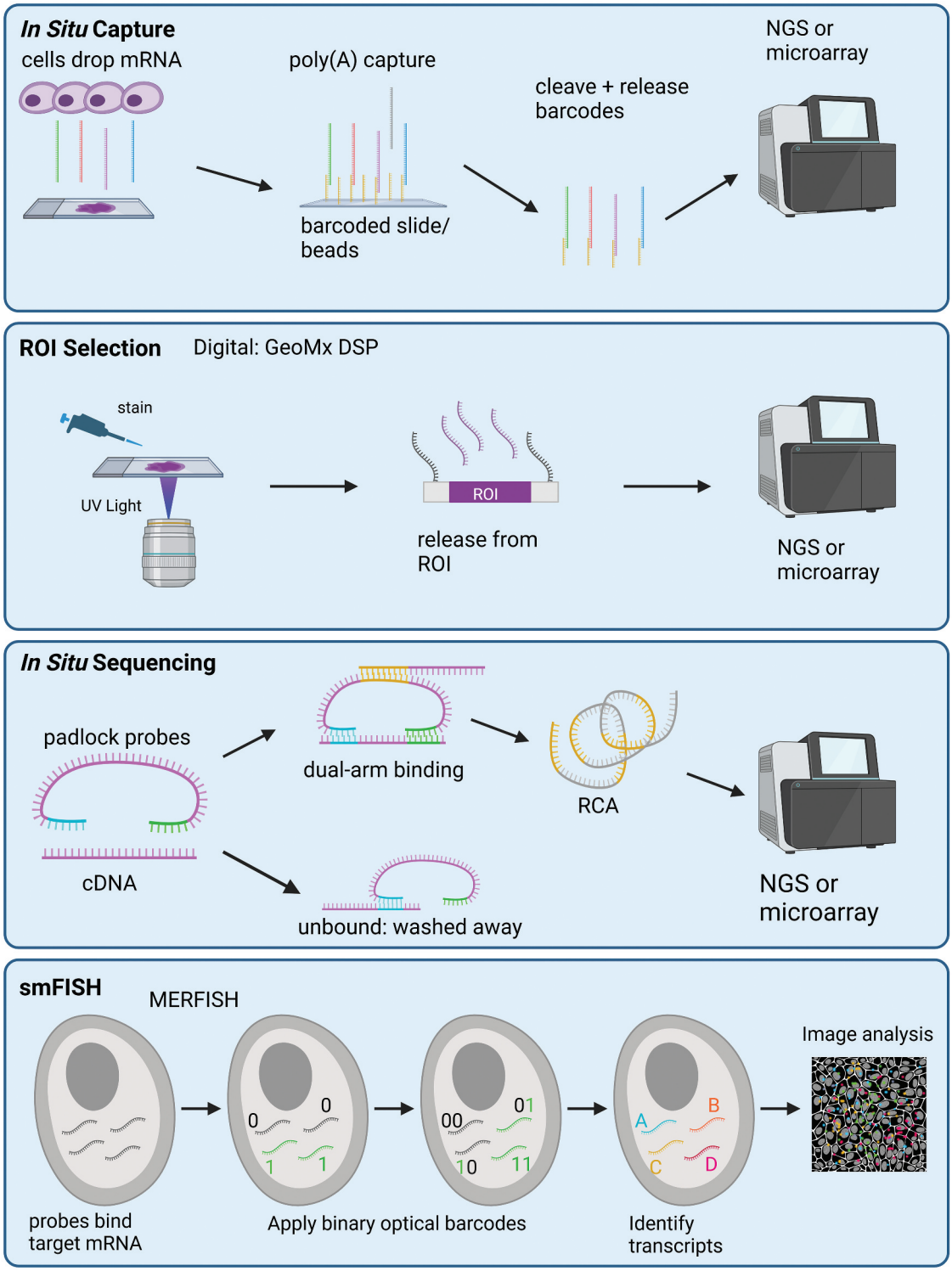

Figure 2. Schematics of popular spatial transcriptomic techniques. Top panel: in situ capture—cells drop RNA onto barcoded slide where mRNA molecules are captured by their poly(A) tail (or through gene panels). Barcodes are cleaved from the slide to release mRNA and sequenced to determine gene and spatial location. Second panel: ROI selection—an example of digital ROI selection using GeoMx DSP where samples are stained and imaged with UV light to release photocleavable probes for sequencing. Third panel: in situ sequencing: padlock probes bind dual arms to cDNA targets, which then undergo rolling circle amplification before sequencing. Bottom panel: single-molecule fluorescent in situ hybridization—example of MERFISH, where probes bind targets, followed by multiple rounds of fluorescent barcoding to distinguish probes at subcellular level. Abbreviations: NGS = next generation sequencing; DSP = digital spatial profiling; UV = ultraviolet; ROI = region-of-interest; LCM = laser capture microdissection; RCA = rolling circle amplification; smFISH = single-molecule fluorescent in situ hybridization; MERFISH = multiplex error-robust fluorescent in situ hybridization.

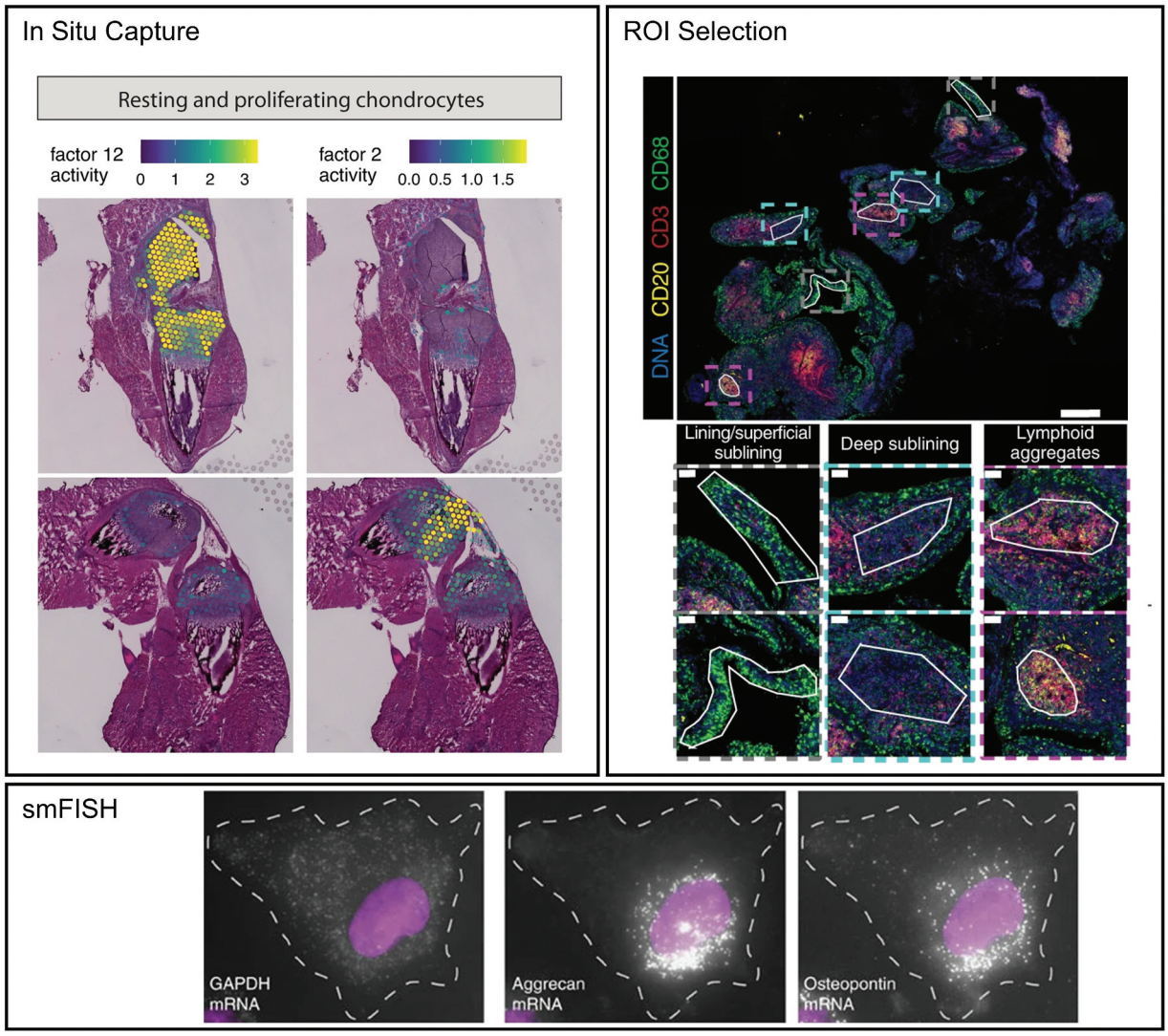

Figure 3. Examples of data collected via various spatial transcriptomic methods. Top left panel: in situ capture results cartilage tissue using RNA rescue spatial transcriptomics[58]. Top right panel: example of selecting regions for GeoMx DSP analysis in synovial tissue[64]. Immunohistochemistry markers inform region selection to match with downstream whole-transcriptome sequencing. Bottom panel: example of single-molecule fluorescent in situ hybridization (smFISH) mapping housekeeping, cartilage (aggrecan), and bone (osteopontin) gene expression at the subcellular level[65]. Images reproduced from references cited under creative commons license 4.0.

are shown in Figure 3. Key findings from the use of spatial transcriptomics on musculoskeletal tissues are listed in Table 3.

In situ capture

In situ capture methods were first developed as "spatial transcriptomics" to allow both the visualization and quantitation of the whole transcriptome with histological context[18]. The original methods printed barcodes on slides that maintained spatial information, a unique molecular identifier, and a poly(T) region to capture mRNA with poly(A) tails. The mRNA is released from tissue sections and captured by barcodes that can later be cleaved and collected for NGS to analyze the transcriptome. In situ capture methods also allow histology and immunohistochemistry to be performed on the tissue section to correlate protein and mRNA expression. The Stahl method of spatial transcriptomics has been further developed and commercialized as 10X Visium. Additional in situ capture methods use beads spread on slides (Slide-Seq[66] or etched wells in slides (high-definition spatially resolved transcriptomics[67] rather than barcodes to capture the mRNA. One method, Stereo-seq uses DNA nanoballs as small as 0.22 μm with spacing 0.5–0.7 μm apart to achieve high spatial resolution[19]. NGS barcoding exhibits low efficiency, with spatial transcriptomics detecting 6.9% as many unique molecular identifiers as transcript spots, comparable to scRNA-seq efficiency (3–25%).

Table 3. Summary of spatial transcriptomics findings on musculoskeletal tissues.

Tissue	Species	Model	Key Findings	Ref
Bone	Mice	Cranial suture formation	Identified distinctive BMP and TGF-β signaling patterns and uncovered the regulatory influence of sensory nerves through Fstl1	38
Bone	Mice	Femur	Identified cortical and trabecular bone markers and used deconvolution to map scRNA-Seq data onto the Visium spots	41
Bone	Mice	Fracture Callus; MDA-MB-231 cell invasion	Localized markers of hard and soft callus and identified DEGs modulated by MDA-MB-231 cell invasion within each zone	40
Bone	Mice	Femur Defect	Identified mostly bone formation-related gene expression in high-strain areas and bone resorption-related gene expression in low-strain environments	39
Cartilage	Mice	4 and 11 days old; SOC formation	Identified novel markers in SOC (Plxnd1, Ccl9, Basp1, and Apln) and SOC adjacent tissue (Msmp)	58
Cartilage; Bone	Mice	Embryonic Development	Adgrg6 is essential for maintaining chondrocyte homeostasis (via SOX9); loss of Adgrg6 leads to activation of IHH signaling and ossification	42
Engineered Cartilage	Bovine	MSC chondrogenesis	Aggrecan mRNA counts did not correlate with chondrogenic matrix deposition, and there is an overlap in gene expression for all markers between MSCs with high and low chondrogenic potential	65
Engineered Cartilage; Cartilage	Rats	Published Dataset[19] MSC Chondrogenesis Articular Cartilage Defect Model	Identified a spatial pattern between TRPV4-YAP-Akt during development using MOSTA[19] and confirmed TRPV4-YAP-Akt pathway regulates collagen synthesis	59
Enthesis	Mice	Supraspinatus enthesis development; p1, p7, p14, p28	Identified Mfge8 and Tnn as novel driving genes of enthesis development	60
Intrafratellar Fat Pad	Human	Osteoarthritis	Identified five sub-clusters of IFP fibroblasts based on OA, sex, and obesity status	43
Ligament	Human	ACL healthy vs degenerated (osteoarthritis patients)	Identified fibroblast subpopulations that increased in diseased ACL, which were found adjacent to endothelial and immune cells	44
Nucleus Pulposus	Mice	Axial skeleton development; E11.5, E12.5	Identified novel chondrogenic cell populations that regulated extracellular matrix homeostasis	45
Nucleus Pulposus	Mice	Intervertebral disk development	Identified that Ctsk+ NPPCs are rare and predominantly located in the outer NP subpopulation and that the common marker Tie2 is not expressed in NP subpopulation or NPPCs	62
Shoulder; Hip; Knee; Cranium	Human	Skeletal development; 5–11 weeks after conception	Developed ISS-Patcher method to infer cell labels from snRNASeq data onto spatial map and identified HIC1+ mesenchymal and dermal fibroblasts in human and SOX9+ Schwann cells in cartilage	63
Spine	Human	Embryonic Development	Mapped HOX gene expression during development and identified antisense gene HOXB-AS3 as a marker for the cervical region in osteochondral, tendon, and fibrous cells	61
Synovium	Human	Rheumatoid Arthritis	The adaptive immune response profile of RA exhibited an abundance of central memory T cells, while effector memory T cells dominated in areas of tissue repair	46
Synovium	Human	Rheumatoid Arthritis	The combination of TNF, IFN-γ, and IL-1β drove the formation of four distinct FLS subtypes; IL-1β was produced by S100A8+ macrophages in the synovial lining	47
Synovium	Human	Rheumatoid Arthritis	Memory B cells co-localize with other B cells, T peripheral or follicular helper cells, CCR7+ T cells, and GZMK+ T cells, but not with fibroblasts or monocytes	61
Synovium	Human	Rheumatoid Arthritis	The FGF pathway was activated via FGF10 and FGFR1 in relapsed RA, which exhibited therapeutic potential in a collagen-induced RA rat model	49
Synovium	Human	Rheumatoid Arthritis	Identified four major clusters in 3D space using consecutive sections	50
Synovium	Human	Rheumatoid Arthritis	Identified a novel tissue-remodeling ITGA5+ fibroblast that induces helper T cells via TGF-β1 in active and lympho-myeloid type RA	51
Synovium	Human	Rheumatoid Arthritis	Confirmed that a DKK3+ fibroblast subpopulation was higher in refractory patients than responders and fibroblast marker FAP was upregulated in deep sublining for refractory patients	64
Tendon	Human	Healthy and diseased supraspinatus tendon	Stromal cells modulate immune function through MIF signaling and APP expression decreased in diseased tenocytes, correlating with decreased LYVE1 expression in macrophages	52
Tendon	Human	Healthy hamstring tendon	MKX+ fibroblasts express collagen matrix, but PDGFRA+ fibroblasts express elastic fiber components	56
Tendon	Human	Supraspinatus tendon; healthy vs diseased	Diseased tenocytes correlated with periostin expression	55
Tendon	Mice	Flexor tendon injury model	Traced tendon fibroblast differentiation into reactive, fibrotic, and synthetic lineages after injury	54
Tendon	Mice	Published Dataset[54]	Identified an area enriched with TRAP expression and developed targeted nanoparticles with TRAP binding peptide for localized tendon delivery	57
Tendon	Rats	Healthy patellar tendon	Identified two tendon fibroblast populations, one in the midsubstance and the other along the periphery, along with a novel spatially regulated gene (AABR07000398.1)	53
Whole Embryo	Mice	Development; e9.5-e16.5	Lineage tracing with sub-cellular resolution of mesoderm → sclerotome → cartilage → bone	19

Abbreviations: 3D = 3 dimensional; AABR0700398.1 = novel spatially regulated gene of unknown function; ACL = anterior cruciate ligament; Adgrg6 = Adhesion G Protein-Coupled Receptor G6; Akt = AKT serine-threonine protein kinase; Apln = Apelin; APP = Amyloid Beta Precursor Protein; Basp1 = Brain Abundant Membrane Attached Signal Protein 1; BMP = bone morphogenic protein; Ccl9 = C-C Motif Chemokine Ligand 9; CCR7 = C-C motif chemokine receptor 7; Ctsk = Cathepsin K; DEG = Differentially Expressed Gene; DKK3 = Dickkopf WNT signaling pathway inhibitor 3; E11.5–12.5 = embryonic stage; FAP = fibroblast activation protein alpha; FGF = fibroblast growth factor; FGFR1 = FGF receptor 1; FLS = Fibroblast-like synoviocytes; Fstl1 = Follistatin Like 1; GZMK = granzyme K positive; HIC1 = hIC ZBTB Transcriptional Repressor 1; Hox = homeobox; IFN-γ = interferon gamma; IFP = intrafratellar fat pad; IHH = Indian hedgehog; IL-1β = interleukin 1 beta; ISS = in situ sequencing; ITGA5 = Integrin Subunit Alpha 5; LYVE1 = Lymphatic Vessel Endothelial Hyaluronan Receptor 1; Mfge8 = milk fat globule-EGF factor 8 protein; MIF = Macrophage Migration Inhibitory Factor; MKX = mohawk; MOSTA = mouse organogenesis spatial tissue atlas; MSC = mesenchymal stem cell; Msmp = Microseminoprotein, Prostate Associated; NP = nucleus pulposus; NPPC = nucleus pulposus progenitor cell; OA = osteoarthritis; PDGFRA = Platelet Derived Growth Factor Receptor Alpha; Plxnd1 = Plexin D1; RA = rheumatoid arthritis; S100A8 = S100 calcium binding protein A8; scRNA-Seq = single-cell RNA sequencing; snRNA-Seq = single-nucleus RNA sequencing; SOC = secondary ossification center; SOX9 = SRY-Box Transcription Factor 9; TGF-β = transforming growth factor beta; Tie2 = TEK Receptor Tyrosine Kinase; TNF = tumor necrosis factor; Tnn = tenascin N; TRAP = tartrate-resistant acid phosphatase; TRPV4 = transient receptor potential cation channel vanilloid 4; YAP = yes-associated protein.

Although being the most popular spatial transcriptomics method, the 10X Visium spatial barcoding has the lowest spatial resolution. With a resolution limited to 55 µm dots spaced 100 µm from center to center, Visium is unable to achieve single-cell resolution. In early 2024, 10X released an improved version, Visium HD, which now uses 2 µm x 2 µm squares for the barcodes with no space in between and can achieve single-cell resolution while still offering the capability of sequencing the whole genome. Currently, Visium HD is available for fresh frozen, fixed frozen, and formalin-fixed, paraffin-embedded (FFPE) tissue sections.

Concerning tissue preparation, most techniques are suitable for frozen sections, with some compatibility for FFPE. However, detection is lower in FFPE due to crosslinking and RNA fragmentation. Any tissue with viable mRNA can be used, but optimization for each tissue is necessary for quality RNA capture. Tissue sections are susceptible to tears, disrupting spatial information and causing RNA loss. Visium slides offer up to 4 spots per slide for replicates, with cost considerations. For frozen sections, a minimum thickness of 10 µm is recommended. Optimization of tissue preparation is needed for each technique. The dense and heterogeneous nature of bone and joint structures requires specialized techniques to capture the spatial intricacies of gene expression accurately. Musculoskeletal tissues are often dense with extracellular matrix proteins and many tissues are hypocellular, which can limit RNA extraction. Bone needs to be demineralized for many histology options, which could damage RNA[29,68]. The calcified bone tissue samples often detach from slides during washes. Wehrle et al developed a protocol that takes 18 days (mostly for decalcification) to reliably perform Visium on mouse bone samples, even with muscle tissue attached to the bone. To achieve DV_{200} ratios > 50% (i.e., > 50% of RNA are larger than 200 bases), which is needed for Visium, Wherle et al recommend optimizing the minimum required decalcification time to section samples to 5 µm, avoiding long-term storage, and using sterile instruments and RNase-Away during sectioning[69]. While many methods use fresh frozen tissue, it has recently been demonstrated that in muscle tissue from the myotendinous junction, spatial transcriptomics can produce quality data from tissue samples that have been stored at −80°C for six years[69], so older samples can be used if stored properly.

A new spatial transcriptomics method termed RNA-Rescue Spatial Transcriptomics (RRST) can increase RNA quality and capture[58]. Traditional Visium spatial transcriptomics relies on fresh frozen tissue with RNA integrity number (RIN) > 7, but later adaptations used a gene panel instead of poly(A) capture to perform Visium on FFPE samples. RRST employs a similar gene panel strategy with formalin fixation of frozen sections to implement the Visium protocol. When tested on cartilage at the end of mouse long bones at postnatal days 4 (P4) and 11 (P11), RRST found a 3-to-9-fold increase in unique genes compared to standard Visium (1298 and 1750 unique genes compared to < 100)[58]. Investigations in other tissues (brain, prostate cancer, colon) confirmed improved RNA capture and more unique genes identified using RRST versus traditional Visium for samples with both low- and high-quality RIN values.

Recently, traditional 2D spatial transcriptomics has been advanced to achieve 3D capability[50]. The method re-creates a 3D tissue structure with histological and spatial transcriptomic information by collecting consecutive tissue sections and aligning the images.

In situ sequencing

In situ sequencing (ISS) enables the direct sequencing of RNA within intact tissues, which maintains histological context. ISS uses padlock probes, rolling-circle amplification, and sequencing-by-ligation chemistry[24]. Each padlock probe has two arms, both of which must bind to its specific target for hybridization to enable rolling circle PCR amplification and detection. 10X genomics offers ISS spatial transcriptomics through their Xenium platform (formerly Cartana). ISS methods are highly sensitive and high throughput, even for low-expressing transcripts. ISS methods offer subcellular resolution for up to 1000 genes. Although ISS methods do not cover the whole transcriptome, the ISS-Patcher R package has been developed to interpolate scRNA-seq data to the spatial locations identified using ISS panels[63]

In situ sequencing is a relatively new method and has not been widely adopted to study musculoskeletal tissues. To the best of our knowledge, we have performed the first 10X Xenium spatial transcriptomics on musculoskeletal tissues on mouse whole knee joints (Figure 4). The preliminary (unpublished) data shows transcripts of five genes (osteocalcin (*Bglap)*, lubricin (*Prg4)*, aggrecan (*Acan)*, cartilage oligomatrix protein (*Comp)*, and myozenin 1 (*Myzo1*) in a healthy mouse knee joint (Figure 4A). This study reveals *Comp*, *Prg4*, and *Acan* expression in cells throughout the meniscus (Figure 4B), and osteocalcin expression in cells along the contour of the bone in the trabeculae (Figure 4C).

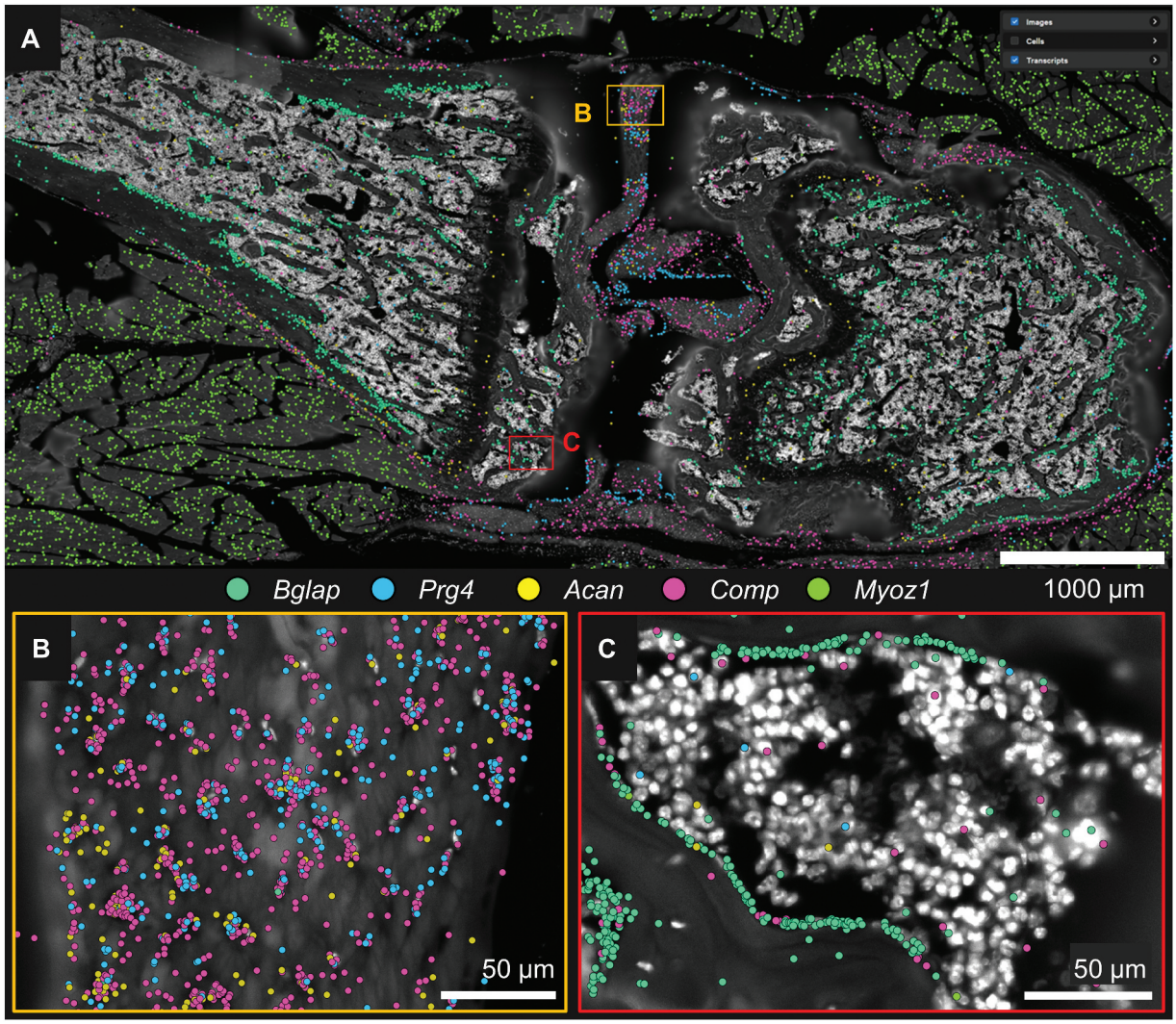

Figure 4. Example (unpublished data) of 10X xenium in situ sequencing (ISS) on a healthy 12-week old mouse knee joint (A) showing transcripts for osteocalcin (*Bglap*), lubricin (*Prg4*), aggrecan (*Acan*), cartilage oligomatrix protein (*Comp*), and myozenin 1 (*Myoz1*). Scale bar is 1000 µm. Zoomed in panels of the meniscus (B) and trabeculae in bone (C). Scale bar is 50 µm.

ROI selection

ROI selection methods use physical or digital means to determine an ROI in a tissue sample where the mRNA is captured and then analyzed via cDNA microarray, bulk RNA sequencing (RNA-Seq), or scRNA-Seq. NanoString offers a digital ROI selection method, GeoMx DSP, where the ROI is illuminated using ultraviolet light to capture photocleavable barcoded genes[20]. The captured genes from the ROI can then be sequenced using RNA-Seq or NanoString nCounter Analysis System. The GeoMx system does not rely on poly-adenylation (poly(A)) capture but gene panels instead. NanoString offers multiple gene panels, including whole-transcriptome panels for both mice and humans, with down to 10 µm in spatial resolution. GeoMx DSP is a commercially available method of digital ROI selection-based spatial transcriptomics. However, GeoMx DSP has not been widely adopted yet for studying musculoskeletal tissues, appearing in only one study of rheumatoid arthritis[64].

Single molecule fluorescent in situ hybridization methods

Single molecule fluorescent in situ hybridization (smFISH) based methods utilize high levels of multiplexing to increase the number of genes analyzed. An early prototype of smFISH methods called sequential Fluorescence In Situ Hybridization (seqFISH) used super-resolution microscopy and combinations of fluorophores to detect up to 32 genes simultaneously at single cell resolution[37]. This method was soon

improved as seqFISH+, which barcoded genes via sequential rounds of hybridization with fluorophores to reach full coverage of the human genome within 8 rounds of hybridization[70]. Another method, multiplexed error-robust FISH (MERFISH)[23] uses a binary barcoding strategy that removes fluorophores only—not FISH probes—that can cover ~ 10,000 genes in less time than seqFISH+[71]. Vizgen offers a commercial MERFISH platform with subcellular resolution and high sensitivity. Most smFISH methods cover hundreds of genes, although higher gene counts are possible, and they achieve subcellular resolution. MERFISH can achieve subcellular resolution, similar to Xenium, while sequencing up to 65,536 genes via multiplexing, covering the whole transcriptome as well. MERFISH has limited imaging time, requiring a 60X lens and imaging for up to 8 rounds of multiplexing for each field of view. Multiplexed smFISH techniques excel in detection efficiency (~100%), but repeated rounds of hybridization may reduce efficiency. Villaseñor et al., improved RNA quality, sensitivity, and specificity for ISH spatial transcriptomics methods by fixing tissue in 4% paraformaldehyde for 24 hours, followed by immersion in 0.5 M ethylenediaminetetraacetic acid (EDTA) for 1–2 weeks[72]. Additionally, pre-treating the slides by incubating for 4 h at 60°C in TEG buffer (25 mm of Tris-HCl at pH 8, 10 mm of EDTA, and 50 mm of glucose) and extended protease treatment improve probe penetration and specificity for ISH methods. While tested on tendon samples, this method should also help other matrix-rich tissues, such as bone, cartilage, and ligament[72].

Conclusions

Spatial transcriptomics has emerged as a powerful tool, offering unprecedented insights into the spatial organization of gene expression within tissues. As technologies continue to evolve, the application of spatial transcriptomics in studying musculoskeletal tissues holds great promise, paving the way for a deeper understanding of musculoskeletal biology and potential therapeutic interventions. Imaging-based methods, such as MERFISH, smFISH, and Xenium may be better for hypothesis testing as they generally have subcellular resolution but sequence fewer genes. Sequencing methods such as Visium or GeoMx may be better for untargeted, shotgun approaches that can generate useful hypotheses from the spatial data from unimpaired tissue sections. Spatial transcriptomics is compatible with histology, and methods (such as Visium) have a fast turnaround and are user-friendly. As further improvements to the techniques are developed to improve spatial resolution and RNA capture, spatial transcriptomic methods could become useful for clinical diagnostics and precision medicine approaches.

Disclosure statement

Board Member, Equity & Stocks in Tesio Pharmaceuticals – DRH, JHNY. Editorial Board: The Journal of Cartilage & Joint Preservation, Cartilage Journal, & the Journal of Orthopedic Research – DRH.

Funding

This work was supported by the National Institutes of Health under [Grant R21AR083189].

ORCID

Thomas L. Jenkins http://orcid.org/0000-0001-8462-7510
Jasper H.N. Yik http://orcid.org/0000-0001-7532-629X
Dominik R. Haudenschild http://orcid.org/0000-0001-9947-9864

References

1. Cieza A, Causey K, Kamenov K, Hanson SW, Chatterji S, Vos T. Global estimates of the need for rehabilitation based on the global burden of disease study 2019: a systematic analysis for the global burden of disease study 2019. Lancet. 2021;396(10267):2006–2017. doi:10.1016/S0140-6736(20)32340-0.
2. Diseases GBD, Injuries C, Abbafati C, Abbas KM, Abbasi M, Abbasifard M, Abbasi-Kangevari M, Abbastabar H, Abd-Allah F, Abdelalim A, et al. Global burden of 369 diseases and injuries in 204 countries and territories, 1990–2019: a systematic analysis for the global burden of disease study 2019. The Lancet. 2020;396(10258):1204–1222. doi:10.1016/S0140-6736(20)30925-9.
3. Collaborators GBDO, Culbreth GT, Haile LM, Rafferty Q, Lo J, Fukutaki KG, Cruz JA, Smith AE, Vollset SE, Brooks PM. Global, regional, and national burden of osteoarthritis, 1990–2020 and projections to 2050: a systematic analysis for the global burden of disease study 2021. The Lancet Rheumatol. 2023;5(9):e508–e522. doi:10.1016/S2665-9913(23)00163-7.
4. Chen D, Shen J, Zhao W, Wang T, Han L, Hamilton JL, Hj I. Osteoarthritis: toward a comprehensive understanding of pathological mechanism. Bone Res. 2017;5(1). doi:10.1038/boneres.2016.44.
5. Yuan C, Pan Z, Zhao K, Li J, Sheng Z, Yao X, Liu H, Zhang X, Yang Y, Yu D, et al. Classification of four distinct osteoarthritis subtypes with a knee joint tissue transcriptome atlas. Bone Res. 2020;8(1):38. doi:10.1038/s41413-020-00109-x.

6. Man GS, Mologhianu G. Osteoarthritis pathogenesis - a complex process that involves the entire joint. J Med Life. 2014;7(1):37–41.
7. Solanki K, Shanmugasundaram S, Shetty N, Kim SJ. Articular cartilage repair & joint preservation: a review of the current status of biological approach. J Clin Orthop Trauma 2021:22(101602.10.1016/j.jcot.2021.101602.
8. Pandey A, Bhutani N. Profiling joint tissues at single-cell resolution: advances and insights. Nat Rev Rheumatol. 2024;20(1):7–20. doi:10.1038/s41584-023-01052-x.
9. Wang T, Wang L, Zhang L, Long Y, Zhang Y, Hou Z. Single-cell rna sequencing in orthopedic research. Bone Res. 2023;11(1):10. doi:10.1038/s41413-023-00245-0.
10. Rai MF, Wu CL, Capellini TD, Guilak F, Dicks AR, Muthuirulan P, Grandi F, Bhutani N, Westendorf JJ. Single cell omics for musculoskeletal research. Curr Osteo Rep. 2021;19(2):131–140. doi:10.1007/s11914-021-00662-2.
11. Saliba AE, Westermann AJ, Gorski SA, Vogel J. Single-cell rna-seq: advances and future challenges. Nucleic Acids Res. 2014;42(14):8845–8860. doi:10.1093/nar/gku555.
12. Gu Y, Hu Y, Zhang H, Wang S, Xu K, Su J. Single-cell rna sequencing in osteoarthritis. Cell Prolif. 2023;56(12):e13517. doi:10.1111/cpr.13517.
13. De Micheli AJ, Swanson JB, Disser NP, Martinez LM, Walker NR, Oliver DJ, Cosgrove BD, Mendias CL. Single-cell transcriptomic analysis identifies extensive heterogeneity in the cellular composition of mouse achilles tendons. Am J Physiol Cell Physiol. 2020;319(5):C885–C894. doi:10.1152/ajpcell.00372.2020.
14. Kendal AR, Layton T, Al-Mossawi H, Appleton L, Dakin S, Brown R, Loizou C, Rogers M, Sharp R, Carr A. Multi-omic single cell analysis resolves novel stromal cell populations in healthy and diseased human tendon. Sci Rep. 2020;10(1):13939. doi:10.1038/s41598-020-70786-5.
15. Kannus P. Structure of the tendon connective tissue. Scand J Med Sci Sports. 2000;10(6):312–320. doi:10.1034/j.1600-0838.2000.010006312.x.
16. Thorpe CT, Screen HR. Tendon structure and composition. Adv Exp Med And Biol. 2016;920:3–10.
17. Moses L, Pachter L. Museum of spatial transcriptomics. Nat Methods. 2022;19(5):534–546. doi:10.1038/s41592-022-01409-2.
18. Stahl PL, Salmen F, Vickovic S, Lundmark A, Navarro JF, Magnusson J, Giacomello S, Asp M, Westholm JO, Huss M, et al. Visualization and analysis of gene expression in tissue sections by spatial transcriptomics. Science. 2016;353(6294):78–82. doi:10.1126/science.aaf2403.
19. Chen A, Liao S, Cheng M, Ma K, Wu L, Lai Y, Qiu X, Yang J, Xu J, Hao S, et al. Spatiotemporal transcriptomic atlas of mouse organogenesis using DNA nanoball-patterned arrays. Cell. 2022;185(10):1777–1792. doi:10.1016/j.cell.2022.04.003.
20. Merritt CR, Ong GT, Church SE, Barker K, Danaher P, Geiss G, Hoang M, Jung J, Liang Y, McKay-Fleisch J, et al. Multiplex digital spatial profiling of proteins and rna in fixed tissue. Nat Biotechnol. 2020;38(5):586–599. doi:10.1038/s41587-020-0472-9.
21. Femino AM, Fay FS, Fogarty K, Singer RH. Visualization of single rna transcripts in situ. Science. 1998;280(5363):585–590. doi:10.1126/science.280.5363.585.
22. Haimovich G, Gerst JE. Single-molecule fluorescence in situ hybridization (smfish) for rna detection in adherent animal cells. Bio Protoc. 2018;8(21):e3070. doi:10.21769/BioProtoc.3070.
23. Chen KH, Boettiger AN, Moffitt JR, Wang S, Zhuang X. Rna imaging. Spatially resolved, highly multiplexed rna profiling in single cells. Science. 2015;348(6233):aaa6090. doi:10.1126/science.aaa6090.
24. Ke R, Mignardi M, Pacureanu A, Svedlund J, Botling J, Wahlby C, Nilsson M. In situ sequencing for rna analysis in preserved tissue and cells. Nat Methods. 2013;10(9):857–860. doi:10.1038/nmeth.2563.
25. Achim K, Pettit JB, Saraiva LR, Gavriouchkina D, Larsson T, Arendt D, Marioni JC. High-throughput spatial mapping of single-cell rna-seq data to tissue of origin. Nat Biotechnol. 2015;33(5):503–509. doi:10.1038/nbt.3209.
26. Satija R, Farrell JA, Gennert D, Schier AF, Regev A. Spatial reconstruction of single-cell gene expression data. Nat Biotechnol. 2015;33(5):495–502. doi:10.1038/nbt.3192.
27. Karaiskos N, Wahle P, Alles J, Boltengagen A, Ayoub S, Kipar C, Kocks C, Rajewsky N, Zinzen RP. The drosophila embryo at single-cell transcriptome resolution. Science. 2017;358(6360):194–199. doi:10.1126/science.aan3235.
28. Pandey RV, Schlotterer C, Yan W. Distmap: a toolkit for distributed short read mapping on a hadoop cluster. PLOS ONE. 2013;8(8):e72614. doi:10.1371/journal.pone.0072614.
29. Belluoccio D, Rowley L, Little CB, Bateman JF, Beier F. Maintaining mrna integrity during decalcification of mineralized tissues. PLOS ONE. 2013;8(3):e58154. doi:10.1371/journal.pone.0058154.
30. Chau M, Lui JC, Landman EB, Spath SS, Vortkamp A, Baron J, Nilsson O, Marcu KB. Gene expression profiling reveals similarities between the spatial architectures of postnatal articular and growth plate cartilage. PLOS ONE. 2014;9(7):e103061. doi:10.1371/journal.pone.0103061.
31. Garrison P, Yue S, Hanson J, Baron J, Lui JC, Klymkowsky M. Spatial regulation of bone morphogenetic proteins (bmps) in postnatal articular and growth plate cartilage. PLOS ONE. 2017;12(5):e0176752. doi:10.1371/journal.pone.0176752.
32. Lui JC, Chau M, Chen W, Cheung CS, Hanson J, Rodriguez-Canales J, Nilsson O, Baron J. Spatial regulation of gene expression during growth of articular cartilage in juvenile mice. Pediatr Res. 2015;77(3):406–415. doi:10.1038/pr.2014.208.
33. McAlinden A, Varghese N, Wirthlin L, Chang LW, Engler AJ. Differentially expressed micrornas in chondrocytes from distinct regions of developing human cartilage. PLOS ONE. 2013;8(9):e75012. doi:10.1371/journal.pone.0075012.

34. Nguyen JKB, Gomez-Picos P, Liu Y, Ovens K, Eames BF. Common features of cartilage maturation are not conserved in an amphibian model. Dev Dyn. 2023;252 (11):1375–1390. doi:10.1002/dvdy.594.
35. Tanaka N, Tashiro T, Katsuragawa Y, Sawabe M, Furukawa H, Fukui N. Expression of minor cartilage collagens and small leucine rich proteoglycans may be relatively reduced in osteoarthritic cartilage. BMC Musculoskelet Disord. 2019;20(1):232. doi:10.1186/s12891-019-2596-y.
36. Xin X, Jiang X, Lichtler A, Kronenberg M, Rowe D, Pachter JS. Laser-capture microdissection and rna extraction from perfusion-fixed cartilage and bone tissue from mice implanted with human ipsc-derived mscs in a calvarial defect model. Methods Mol Biol. 2018;1723:385–396.
37. Lubeck E, Cai L. Single-cell systems biology by super-resolution imaging and combinatorial labeling. Nat Methods. 2012;9(7):743–748. doi:10.1038/nmeth.2069.
38. Tower RJ, Li Z, Cheng YH, Wang XW, Rajbhandari L, Zhang Q, Negri S, Uytingco CR, Venkatesan A, Zhou FQ, et al. Spatial transcriptomics reveals a role for sensory nerves in preserving cranial suture patency through modulation of BMP/TGF-β signaling. Proc Natl Acad Sci USA. 2021;118(42). doi:10.1073/pnas.2103087118.
39. Mathavan N, Singh A, Marques FC, Gunther D, Kuhn GA, Wehrle E, Muller R. Spatial transcriptomics in bone mechanomics: exploring the mechanoregulation of fracture healing in the era of spatial omics. Sci Adv. 2025;11(1):eadp8496. doi:10.1126/sciadv.adp8496.
40. Jiang W, Caruana DL, Back J, Lee FY. Unique spatial transcriptomic profiling of the murine femoral fracture callus: a preliminary report. Cells 2024:Cells. 2024;13 (6):522. doi:10.3390/cells13060522.
41. Xiao X, Juan C, Drennon T, Uytingco CR, Vishlaghi N, Sokolowskei D, Xu L, Levi B, Sammarco MC, Tower RJ. Spatial transcriptomic interrogation of the murine bone marrow signaling landscape. Bone Res. 2023;11 (1):59. doi:10.1038/s41413-023-00298-1.
42. Bian F, Hansen V, Feng HC, He J, Chen Y, Feng K, Ebrahimi B, Gray RS, Chai Y, Wu CL, et al. The g protein-coupled receptor adgrg6 maintains mouse growth plate homeostasis through ihh signaling. J Bone Min Res. 2024;39(11):1644–1658. doi:10.1093/jbmr/zjae144.
43. Peters H, Potla P, Rockel JS, Tockovska T, Pastrello C, Jurisica I, Delos Santos K, Vohra S, Fine N, Lively S, et al. Cell and transcriptomic diversity of infrapatellar fat pad during knee osteoarthritis. Ann Rheumatic Dis. 2025;84(2):351–367. doi:10.1136/ard-2024-225928.
44. Yang R, Xu T, Zhang L, Ge M, Yan L, Li J, Fu W. A single-cell atlas depicting the cellular and molecular features in human anterior cruciate ligamental degeneration: a single cell combined spatial transcriptomics study. Elife. 2023;12:12(. doi:10.7554/eLife.85700.
45. Zhou T, Chen Y, Liao Z, Zhang L, Su D, Li Z, Yang X, Ke X, Liu H, Chen Y, et al. Spatiotemporal characterization of human early intervertebral disc formation at single-cell resolution. Adv Sci (Weinh). 2023;10(14): e2206296. doi:10.1002/advs.202206296.
46. Carlberg K, Korotkova M, Larsson L, Catrina AI, Stahl PL, Malmstrom V. Exploring inflammatory signatures in arthritic joint biopsies with spatial transcriptomics. Sci Rep. 2019;9(1):18975. doi:10.1038/s41598-019-55441-y.
47. Smith MH, Gao VR, Periyakoil PK, Kochen A, Ef D, Goodman SM, Norman TM, Donlin LT, Leslie CS, Rudensky AY. Drivers of heterogeneity in synovial fibroblasts in rheumatoid arthritis. Nat Immunol. 2023;24 (7):1200–1210. doi:10.1038/s41590-023-01527-9.
48. Hardt U, Carlberg K, Af Klint E, Sahlstrom P, Larsson L, van Vollenhoven A, Hernandez Machado S, Israelsson L, Amara K, Chemin K, et al. Integrated single cell and spatial transcriptomics reveal autoreactive differentiated b cells in joints of early rheumatoid arthritis. Sci Rep. 2022;12(1):11876. doi:10.1038/s41598-022-15293-5.
49. Meng X, Chen Z, Li T, Nie Z, Han H, Zhong S, Yin Z, Sun S, Xie J, Shen J, et al. Role and therapeutic potential for targeting fibroblast growth factor 10/fgfr1 in relapsed rheumatoid arthritis. Arthritis Rheumatol. 2024;76(1):32–47. doi:10.1002/art.42674.
50. Vickovic S, Schapiro D, Carlberg K, Lotstedt B, Larsson L, Hildebrandt F, Korotkova M, Hensvold AH, Catrina AI, Sorger PK, et al. Three-dimensional spatial transcriptomics uncovers cell type localizations in the human rheumatoid arthritis synovium. Commun Biol. 2022;5(1):129. doi:10.1038/s42003-022-03050-3.
51. Zheng L, Gu M, Li X, Hu X, Chen C, Kang Y, Pan B, Chen W, Xian G, Wu X, et al. Itga5(+) synovial fibroblasts orchestrate proinflammatory niche formation by remodelling the local immune microenvironment in rheumatoid arthritis. Ann rheumatic Dis. 2025;84 (2):232–252. doi:10.1136/ard-2024-225778.
52. Akbar M, MacDonald L, Crowe LAN, Carlberg K, Kurowska-Stolarska M, Stahl PL, Snelling SJB, Ib M, Millar NL. Single cell and spatial transcriptomics in human tendon disease indicate dysregulated immune homeostasis. Ann rheumatic Dis. 2021;80(11):1494–1497. doi:10.1136/annrheumdis-2021-220256.
53. Steffen D, Mienaltowski M, Baar K. Spatial gene expression in the adult rat patellar tendon. Matrix Biol Plus. 2023;19-20:19–20(100138. doi:10.1016/j.mbplus.2023.100138.
54. Ackerman JE, Best KT, Muscat SN, Pritchett EM, Nichols AEC, Wu CL, Loiselle AE. Defining the spatial-molecular map of fibrotic tendon healing and the drivers of scleraxis-lineage cell fate and function. Cell Rep. 2022;41(8):111706. doi:10.1016/j.celrep.2022.111706.
55. Fu W, Yang R, Li J. Single-cell and spatial transcriptomics reveal changes in cell heterogeneity during progression of human tendinopathy. BMC Biol. 2023;21 (1):132. doi:10.1186/s12915-023-01613-2.
56. Mimpen JY, Ramos-Mucci L, Paul C, Kurjan A, Hulley PA, Ikwuanusi CT, Cohen CJ, Gwilym SE, Baldwin MJ, Cribbs AP, et al. Single nucleus and spatial transcriptomic profiling of healthy human hamstring tendon. Faseb J. 2024;38 (10):e23629. doi:10.1096/fj.202300601RRR.
57. Adjei-Sowah E, Chandrasiri I, Xiao B, Liu Y, Ackerman JE, Soto C, Nichols AEC, Nolan K, Benoit DSW, Loiselle AE. Development of a nanoparticle-based tendon-targeting drug delivery system to pharmacologically

modulate tendon healing. Sci Adv. 2024;10(25):eadn2332. doi:10.1126/sciadv.adn2332.
58. Mirzazadeh R, Andrusivova Z, Larsson L, Newton PT, Galicia LA, Abalo XM, Avijgan M, Kvastad L, Denadai-Souza A, Stakenborg N, et al. Spatially resolved transcriptomic profiling of degraded and challenging fresh frozen samples. Nat Commun. 2023;14(1):509. doi:10.1038/s41467-023-36071-5.
59. Yang Y, Xu Z, He S, Wang C, Li R, Zhang R, Li J, Yang Z, Li H, Liu S, et al. Developmental dynamics mimicking inversely engineered pericellular matrix for articular cartilage regeneration. Biomaterials. 2025;317(123066):123066. doi:10.1016/j.biomaterials.2024.123066.
60. Zhang T, Wan L, Xiao H, Wang L, Hu J, Lu H. Single-cell rna sequencing reveals cellular and molecular heterogeneity in fibrocartilaginous enthesis formation. Elife. 2023;12. doi:10.7554/eLife.85873.
61. Lawrence JEG, Roberts K, Tuck E, Li T, Mamanova L, Balogh P, Usher I, Piapi A, Mazin P, Anderson ND, et al. Hox gene expression in the developing human spine. Nat Commun. 2024;15(1):10023. doi:10.1038/s41467-024-54187-0.
62. Chen Y, Zhang L, Shi X, Han J, Chen J, Zhang X, Xie D, Li Z, Niu X, Chen L, et al. Characterization of the nucleus pulposus progenitor cells via spatial transcriptomics. Adv Sci (Weinh). 2024;11(18):e2303752. doi:10.1002/advs.202303752.
63. To K, Fei L, Pett JP, Roberts K, Blain R, Polanski K, Li T, Yayon N, He P, Xu C, et al. A multi-omic atlas of human embryonic skeletal development. Nature. 2024;635(8039):657–667. doi:10.1038/s41586-024-08189-z.
64. Rivellese F, Surace AEA, Goldmann K, Sciacca E, Cubuk C, Giorli G, John CR, Nerviani A, Fossati-Jimack L, Thorborn G, et al. Rituximab versus tocilizumab in rheumatoid arthritis: synovial biopsy-based biomarker analysis of the phase 4 r4ra randomized trial. Nat Med. 2022;28(6):1256–1268. doi:10.1038/s41591-022-01789-0.
65. Cote AJ, Cm M, Farrell MJ, Pd M, Dunagin MC, Raj A, Mauck RL. Single-cell differences in matrix gene expression do not predict matrix deposition. Nat Commun. 2016;7(1). doi:10.1038/ncomms10865.
66. Rodriques SG, Stickels RR, Goeva A, Martin CA, Murray E, Vanderburg CR, Welch J, Chen LM, Chen F, Ez M. Slide-seq: a scalable technology for measuring genome-wide expression at high spatial resolution. Science. 2019;363(6434):1463–1467. doi:10.1126/science.aaw1219.
67. Vickovic S, Eraslan G, Salmen F, Klughammer J, Stenbeck L, Schapiro D, Aijo T, Bonneau R, Bergenstrahle L, Navarro JF, et al. High-definition spatial transcriptomics for in situ tissue profiling. Nat Methods. 2019;16(10):987–990. doi:10.1038/s41592-019-0548-y.
68. Wehrle E, Gunther D, Mathavan N, Singh A, Muller R. Protocol for preparing formalin-fixed paraffin-embedded musculoskeletal tissue samples from mice for spatial transcriptomics. STAR Protoc. 2024;5(2):102986. doi:10.1016/j.xpro.2024.102986.
69. Ruoss S, Esparza MC, Vasquez-Bolanos LS, Nasamran CA, Fisch KM, Engler AJ, Ward SR. Spatial transcriptomics tools allow for regional exploration of heterogeneous muscle pathology in the pre-clinical rabbit model of rotator cuff tear. J Orthop Surg Res. 2022;17(1):440. doi:10.1186/s13018-022-03326-8.
70. Lubeck E, Coskun AF, Zhiyentayev T, Ahmad M, Cai L. Single-cell in situ rna profiling by sequential hybridization. Nat Methods. 2014;11(4):360–361. doi:10.1038/nmeth.2892.
71. Xia C, Fan J, Emanuel G, Hao J, Zhuang X. Spatial transcriptome profiling by merfish reveals subcellular rna compartmentalization and cell cycle-dependent gene expression. Proc Natl Acad Sci USA. 2019;116(39):19490–19499. doi:10.1073/pnas.1912459116.
72. Villasenor S, Grinstein M. Spatial high-resolution analysis of gene expression levels in tendons. J Vis Exp. 2024;205:e65852. doi:10.3791/65852.

SARTORIUS

BioTechniques
The International Journal of Life Science Methods